

FILE COPY

NO 2



RESTRICTED

Copy 209  
RM L9H18

## RESEARCH MEMORANDUM

LATERAL-CONTROL INVESTIGATION AT A REYNOLDS NUMBER  
OF 5,300,000 OF A WING OF ASPECT RATIO 5.8  
SWEPTFORWARD 32° AT THE LEADING EDGE

By Robert R. Graham

Langley Aeronautical Laboratory  
Langley Air Force Base, Va.

CLASSIFICATION CHANGED TO  
UNCLASSIFIED  
AUTHORITY CROWLEY CHANGE #1922  
DATE 12-14-53 CLASSIFIED DOCUMENT T.C.F.

This document contains classified information affecting the National Defense of the United States within the meaning of the Espionage Act, USC 50:31 and 32. Its transmission or the revelation of its contents in any manner to an unauthorized person is prohibited by law. Information so classified may be imparted only to persons in the military and naval services of the United States, appropriate civilian officers and employees of the Federal Government who have a legitimate interest therein, and to United States citizens of known loyalty and discretion who of necessity must be informed thereof.

THIS DOCUMENT ON LOAN FROM THE FILES OF  
NATIONAL ADVISORY COMMITTEE FOR AERONAUTICS  
LANGLEY AERONAUTICAL LABORATORY  
LANGLEY FIELD, HAMPTON, VIRGINIA  
RETURN TO THE ABOVE ADDRESS  
REQUESTS FOR PUBLICATIONS SHOULD BE ADDRESSED  
AS FOLLOWS:

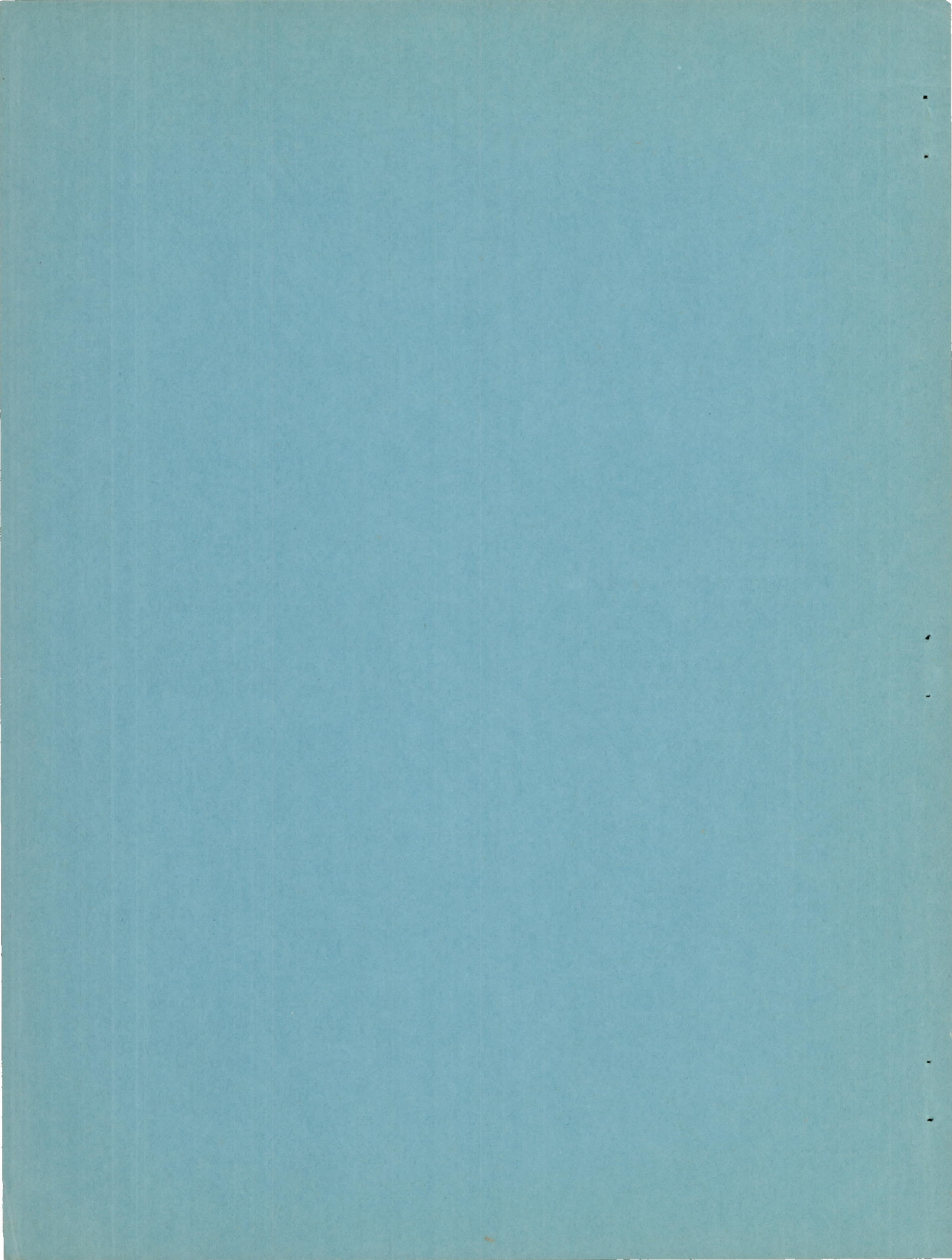
NATIONAL ADVISORY COMMITTEE FOR AERONAUTICS  
1512 M STREET, N. W.  
WASHINGTON 25, D. C.

NATIONAL ADVISORY COMMITTEE  
FOR AERONAUTICS

WASHINGTON

February 7, 1950

RESTRICTED



## NATIONAL ADVISORY COMMITTEE FOR AERONAUTICS

## RESEARCH MEMORANDUM

LATERAL-CONTROL INVESTIGATION AT A REYNOLDS NUMBER  
OF 5,300,000 OF A WING OF ASPECT RATIO 5.8  
SWEPTFORWARD 32° AT THE LEADING EDGE

By Robert R. Graham

## SUMMARY

The low-speed lateral control characteristics of a 32° sweptforward wing of aspect ratio 5.8 and NACA 65-series airfoil sections have been determined in the Langley 19-foot pressure tunnel. The investigation included the measurement of the hinge-moment and normal-force characteristics of an aileron and the rolling-effectiveness characteristics of the aileron and several configurations of spoilers. The effects of an inboard leading-edge flap alone and in combination with a double slotted trailing-edge flap on the characteristics of the aileron and spoilers were also investigated. The tests were made at a Reynolds number of 5,300,000 and a Mach number of 0.16.

The rate of change of rolling-moment coefficient with aileron deflection  $C_{l\delta}$  decreased from 0.00115 at low angles of attack to 0.00060 at maximum lift.

The addition of a leading-edge flap on the inboard portion of the wing resulted in a slight increase in  $C_{l\delta}$  through most of the angle-of-attack range but had a negligible effect at maximum lift. When a partial-span double slotted flap was deflected in combination with the leading-edge flap,  $C_{l\delta}$  did not decrease to as low a value at maximum lift as with flaps neutral.

Spoiler lateral controls located on the inboard portion of the wing were considerably less effective in producing rolling moments than spoilers located near the tips even at low angles of attack where there was no stalling on the wing. A spoiler on the outboard 20 percent of the semispan maintained most of its effectiveness to the highest angle of attack tested. The rolling effectiveness was about the same for a step spoiler as for a plain spoiler.

The spoilers showed the characteristic reverse rolling moments for small projections that have been observed for similarly located spoilers on unswept wings.

#### INTRODUCTION

The use of swept wings to alleviate some of the high-speed aero-dynamic problems of transonic aircraft introduces several stability and control problems in the low-speed range. Some of these problems are the result of the stalling characteristics of the swept wings. Sweeping the wings usually causes the initial stall to occur on the inboard portion of sweptforward wings and on the outboard portion of sweptback wings. The stall is often accompanied by destabilizing pitching moments and, in the case of the sweptback wings, a loss of lateral control.

Leading-edge stall-control devices such as slats, leading-edge flaps, and drooped-nose flaps have been used successfully on sweptback wings to delay the tip stall and thus allow stable pitching-moment variations and lateral control to be maintained throughout the high-lift range. (See references 1 to 3.) Such devices on sweptforward wings, however, would be required to delay the inboard stall to improve the pitching-moment characteristics and, consequently, might cause a loss of lateral control.

In order to determine the effects of stall-control and high-lift devices on the longitudinal stability and lateral control characteristics of a sweptforward wing, an investigation was carried out in the Langley 19-foot pressure tunnel on a  $32^\circ$  sweptforward wing of aspect ratio 5.8 and taper ratio 0.39. The longitudinal stability characteristics of the wing are reported in reference 4, and the lateral control characteristics of the wing are presented herein.

Types of lateral control investigated were an aileron and several configurations of spoilers. Stall-control and high-lift devices investigated with the lateral controls were an inboard leading-edge flap and partial-span and full-span double slotted flaps. The major portion of the investigation was made with the wing installed on a fuselage, but one spoiler configuration was tested on the wing alone.

#### SYMBOLS AND COEFFICIENTS

The data are referred to the wind axes with the origin at 25 percent of the mean aerodynamic chord on the wing alone and 10 percent of the mean aerodynamic chord on the wing-fuselage combination. The data have

been reduced to standard NACA nondimensional coefficients which are defined as follows:

$$C_L \quad \text{lift coefficient} \quad \left( \frac{\text{Lift}}{qS} \right)$$

$$C_D \quad \text{drag coefficient} \quad \left( \frac{\text{Drag}}{qS} \right)$$

$$C_m \quad \text{pitching-moment coefficient} \quad \left( \frac{\text{Pitching moment}}{qS\bar{c}} \right)$$

$$C_l \quad \text{rolling-moment coefficient} \quad \left( \frac{\text{Rolling moment}}{qS_b} \right)$$

$$C_n \quad \text{yawing-moment coefficient} \quad \left( \frac{\text{Yawing moment}}{qS_b} \right)$$

$$C_{h_a} \quad \text{aileron hinge-moment coefficient} \quad \left( \frac{\text{Hinge moment}}{2M_{a_d}} \right)$$

$$C_{N_a} \quad \text{aileron normal-force coefficient} \quad \left( \frac{\text{Normal force}}{qS_a} \right)$$

$$P_R \quad \text{resultant pressure coefficient in aileron balance compartment} \quad \left( \frac{\text{Pressure below seal} - \text{Pressure above seal}}{q} \right)$$

$$E \quad \text{aileron-seal leakage factor} \quad \left( 1 - \frac{\text{Pressure difference across seal}}{\text{Pressure difference across vents}} \right)$$

$$R \quad \text{Reynolds number} \quad \left( \frac{\rho V c}{\mu} \right)$$

$$\alpha \quad \text{angle of attack of root chord line, degrees}$$

$\delta_a$  aileron deflection measured in plane perpendicular to hinge line, positive when deflected down, degrees  
 $\delta_s$  spoiler projection, fraction of local wing chord  
 $\Lambda$  angle of sweep of leading edge  
 $S$  wing area  
 $\bar{c}$  mean aerodynamic chord  $\left( \frac{2}{S} \int_0^{b/2} c^2 dy \right)$   
 $c$  local wing chord parallel to plane of symmetry  
 $c'$  local wing chord perpendicular to  $0.225c$  line  
 $A$  aspect ratio  $\left( \frac{b^2}{S} \right)$   
 $y$  lateral coordinate  
 $b$  wing span perpendicular to plane of symmetry  
 $S_a$  aileron area aft of hinge line (0.701 sq ft)  
 $M_a$  moment of area of aileron aft of hinge line about hinge axis (0.0884 cu ft)  
 $b_s$  spoiler span measured perpendicular to plane of symmetry  
 $c_a$  aileron chord aft of hinge line measured perpendicular to hinge line  
 $c_b$  aileron nose balance chord forward of hinge line measured perpendicular to hinge line  
 $q$  dynamic pressure  $\left( \frac{\rho V^2}{2} \right)$   
 $\rho$  density of air  
 $V$  free-stream velocity  
 $\mu$  coefficient of viscosity

$C_{l\delta}$	rate of change of rolling-moment coefficient with aileron deflection
$C_{h\delta}$	rate of change of aileron hinge-moment coefficient with aileron deflection
$P_{R\delta}$	rate of change of resultant-pressure coefficient with aileron deflection
$C_{h\alpha}$	rate of change of aileron hinge-moment coefficient with angle of attack
$P_{R\alpha}$	rate of change of resultant-pressure coefficient with angle of attack

#### MODEL AND APPARATUS

The model used in the investigation was of steel construction and had an aspect ratio of 5.79, a taper ratio of 0.389, and  $32.3^\circ$  sweep-forward of the leading edge. The general dimensions of the model are shown in figure 1.

The airfoil section perpendicular to the 22.5-percent-chord line (the 25-percent-chord line on the original unswept wing (reference 5)) was an NACA 65-210 profile. The wing had no geometric dihedral and  $1.8^\circ$  geometric washout at the tips. For most of the tests, the wing was installed on a fuselage of circular cross section and a fineness ratio of 12:1, with the root chord line of the wing on the center line of the fuselage.

Details of the lateral-control devices are shown in figure 2. The aileron was of the constant-percentage type ( $0.20c'$  or  $0.222c$ ) and extended from  $0.59\frac{b}{2}$  to  $0.98\frac{b}{2}$  on the left wing panel. It had the same contour behind the hinge line as the corresponding portion of the airfoil section. The nose was cut away so that a flexible seal could be attached at the hinge line and thus any hinge moment due to tension in the seal would be eliminated. The balance compartment was provided with orifices for measuring pressures above and below the seal. The aileron was attached to the wing by three strain-gage beams which indicated electrically the aileron hinge moments and the component of the aileron normal force perpendicular to the wing-chord line.

Two configurations of spoiler lateral controls were investigated. The plain spoiler extended along the 60-percent-chord line, and the step spoiler consisted of a series of spoiler segments placed perpendicular to the plane of symmetry with the midpoint of each segment

on the 60-percent-chord line. The spoilers projected normal to the surface of the wing, and projections investigated were  $0.005c$ ,  $0.010c$ ,  $0.040c$ , and  $0.100c$ . Details of the spoilers are shown in figure 2.

Details of the  $0.41\frac{b}{2}$  leading-edge flap and the partial-span and full-span double slotted flaps are shown in figure 3. The position and deflection of the double slotted flap and fore flap were the same as those used on the unswept wing of reference 5.

A two-support system was used to mount the wing alone in the tunnel, but a third support was added at the rear of the fuselage when the wing-fuselage combination was tested. The model mounted in the tunnel is shown in figure 4.

#### TESTS

The tests were made in the Langley 19-foot pressure tunnel with the air in the tunnel compressed to about  $2\frac{1}{3}$  atmospheres. The Reynolds and Mach numbers for the tests were 5,300,000 and 0.16, respectively.

The effectiveness of the various lateral-control devices was determined by taking force and moment measurements through a range of angle of attack from  $0^\circ$  to beyond the stall with the aileron set at various deflections or with the spoilers set at various heights, spans, and spanwise locations. Aileron hinge moments, normal forces, and balance-compartment pressures were also measured in the aileron tests. One series of spoiler tests was made on the basic wing, but the rest of the tests were made on the wing-fuselage combination. The aileron and spoilers were tested on the wing-fuselage combination with flaps retracted and with inboard leading-edge flaps deflected. In addition, the aileron was tested on the wing-fuselage combination with inboard leading-edge and partial-span double slotted flaps deflected, and the spoilers were tested on the wing-fuselage combination with inboard leading-edge and full-span double slotted flaps deflected.

#### CORRECTIONS TO DATA

The lift and pitching-moment data presented herein have been corrected for air-stream misalignment and for support tare and

interference effects. Jet-boundary corrections to the angle of attack and pitching-moment data were obtained by a method adapted from reference 6 and are as follows:

$$\Delta\alpha = 0.67 C_L$$

$$\Delta C_m = 0.004 C_L$$

No corrections have been applied to the rolling-moment, yawing-moment, hinge-moment, or normal-force data. Jet-boundary corrections to these data were found to be small enough to be negligible, and the tare and interference effects on these data are believed to be negligible.

A calibration of the aileron seal indicated a leakage factor  $E$  of 0.036. The balance-compartment pressures have been corrected for this leakage so that they represent pressures with a complete seal. The effects of the leakage on the rolling-moment and hinge-moment coefficients, however, are believed to be small and have been neglected.

The aileron normal forces were measured normal to the wing-chord line instead of normal to the aileron-chord line as is customary. An analysis of aileron-pressure-distribution data from reference 7, however, indicates that at small deflections very little error is introduced by this method of measurement and at large deflections the normal forces as presented herein are about the same as the true normal forces multiplied by the cosine of the angle of deflection.

#### RESULTS AND DISCUSSION

In order to simplify comparison of the results, the data are presented in the following order. The characteristics of the aileron are presented in figures 5, 6, and 7 for the configurations of flaps neutral, leading-edge flaps deflected, and leading-edge and double slotted flaps deflected, respectively. The data of figures 5 to 7 have been summarized in figures 8 and 9. The characteristics of the spoilers are presented in figures 10 to 13 for both step and plain spoilers on the various model configurations.

## Aileron Characteristics

Wing and fuselage without flaps.— The rolling-effectiveness parameter  $C_{l\delta}$  was constant in the low and moderate angle-of-attack range at about 0.00115 to  $\alpha = 12^\circ$ . (See fig. 8.) Above that angle-of-attack range the value of  $C_{l\delta}$  decreased until at  $\alpha = 25^\circ$  it was only about 0.00060 or one-half the value at  $\alpha = 0^\circ$ . Stall studies (reference 4) show that the initial stall occurred at the root of the wing at a fairly low angle of attack. As the angle of attack was increased, the stalled area spread outward until at about  $12^\circ$  it had reached the inboard end of the aileron. Further increases in angle of attack caused the stall to spread still more until at the highest angle of attack of the tests ( $25^\circ$ ) a large portion of the aileron was within the stalled area and a reduction of  $C_{l\delta}$  resulted at those angles of attack.

The value of  $C_{l\delta}$  for low angles of attack has been calculated by the method given in reference 8. The computed value was 0.00108 or slightly less than the value obtained experimentally. The agreement is considered satisfactory.

The yawing-moment coefficients due to aileron deflection (fig. 5) show about the same trends as would be expected on an unswept wing. When two ailerons are considered deflected oppositely, adverse yawing moments are obtained which are small at low angles of attack and increase as the angle of attack is increased.

The hinge-moment-coefficient data in figure 5 show that the aileron had a slight upfloating tendency at  $\alpha = 0^\circ$ . The variation of hinge-moment coefficient with angle of attack  $C_{h\alpha}$  measured at  $\delta_\alpha = 0^\circ$  increased from about -0.0046 at  $\alpha = 0^\circ$  to about -0.0175 at the highest angle of attack tested (see fig. 8), resulting in a strong upfloating tendency of the aileron at high angles of attack. The variation of hinge-moment coefficient with aileron deflection  $C_{h\delta}$  was about -0.0062 at angles of attack below  $12^\circ$ , and as the angle of attack was increased to  $25^\circ$ , the value of  $C_{h\delta}$  increased to about -0.0090.

Values of  $C_{h\alpha}$  and  $C_{h\delta}$  for low angles of attack have been calculated by the method outlined in reference 9 to give -0.0029 and -0.0066, respectively, as compared to the experimental values given previously.

Wing and fuselage with leading-edge and trailing-edge flaps.—The summary curves of figure 8 show that  $C_{l\delta}$  was increased slightly in the low and moderate angle-of-attack range when the leading-edge flap was extended. At angles of attack above  $20^\circ$ , however, the values of  $C_{l\delta}$  were about the same as for the wing without flaps. The leading-edge flap had practically no effect on the yawing-moment, hinge-moment, and normal-force characteristics of the aileron. The further addition of the partial-span double slotted flaps caused a slight reduction in  $C_{l\delta}$  at low angles of attack but produced an increase at high angles of attack.

The combination of leading-edge and double slotted flaps caused an increase in  $C_{h\delta}$  through the angle-of-attack range and also caused a slight increase in  $C_{h\alpha}$  in the low angle-of-attack range but caused a large decrease in  $C_{h\alpha}$  at angles of attack above  $13^\circ$ . The combination had little effect on the normal-force coefficients.

The yawing-moment coefficient due to equal up and down ailerons was adverse at all angles of attack above  $5^\circ$  when the combination was deflected. (See fig. 7.) The variation of yawing moment with angle of attack for full up and down ailerons ( $50^\circ$  total) was about the same as with flaps neutral.

Effects of a balance and rolling on hinge-moment characteristics.—The hinge-moment parameters  $C_{h\alpha}$  and  $C_{h\delta}$  have been combined into one parameter  $C_{h\delta}'$  by considering the wing in a steady roll at a rate which is proportional to aileron deflection. Values of  $C_{h\delta}'$  were calculated from the equation

$$C_{h\delta}' = C_{h\delta} + \frac{2(\Delta\alpha)_p}{\Delta\delta_a} C_{h\alpha}$$

where

$C_{h\delta}$  ' rate of change of aileron hinge moment with deflection when wing is in a steady roll

$\frac{2(\Delta\alpha)_p}{\Delta\delta_a}$  ratio of effective change in angle of attack to aileron deflection in a steady roll. (The value of  $\frac{2(\Delta\alpha)_p}{\Delta\delta_a}$  was found to be  $-182 C_{l\delta}$  from data given in references 10 and 11.)

The effects of a sealed internal balance were taken into account by the following relations:

$$C_{h\alpha(\text{bal})} = C_{h\alpha} + \frac{1}{2} P_{R\alpha} \left( \frac{c_b}{c_a} \right)^2$$

$$C_{h\delta(\text{bal})} = C_{h\delta} + \frac{1}{2} P_{R\delta} \left( \frac{c_b}{c_a} \right)^2$$

where the subscript bal refers to the aileron with an internal nose balance and  $c_b/c_a$  is the ratio of the nose-balance chord to the aileron chord.

The results of the calculations from figure 9 compared with the test results of figure 8 show that steady rolling reduces  $C_{h\delta}$  for the unbalanced aileron with flaps neutral from -0.0062 to -0.0052 at  $\alpha = 0^\circ$  and causes similar reductions through the angle-of-attack range. Similar reductions are also shown for the other model configurations. The results also show that the balance chord required to reduce the control-stick force to zero in a steady roll is about 55 percent of the aileron chord at low angles of attack and increases to about 62 percent at high angles of attack.

The leading-edge flap had a negligible effect on the hinge-moment characteristics of the balanced aileron in the roll. Deflecting the leading-edge flap and double slotted flap in combination caused an increase in the balance required for zero stick force in a steady roll to about 62 percent at low angles of attack and 65 percent at high angles of attack. Thus, if the aileron is balanced to give desirable

control stick forces at high subsonic speeds, it will be underbalanced at landing-approach speeds with flaps deflected. It is possible that if a wing such as the one tested is applied to a very large airplane, the stick forces might be large in the landing-approach condition.

#### Spoiler Characteristics

Wing without flaps.— The characteristics of the plain spoiler on the wing without fuselage or flaps (fig. 10) indicate that the outer portion of a full-span spoiler was much more effective than the inner portion. Increasing the 0.10c spoiler span from the outer 40 percent to the outer 63 percent of the semispan (a span increase of over 60 percent) increased the rolling moment only about 35 percent at an angle of attack of about  $0^{\circ}$  and less than 35 percent at higher angles of attack. Further inboard extension of the spoiler span from the outer 63 percent to the plane of symmetry resulted in reduced rolling moments even at low angles of attack. At the highest angle of attack investigated ( $24.9^{\circ}$ ), the spoiler became ineffective in producing rolling moments.

Wing and fuselage without flaps.— The addition of a fuselage had a negligible effect on the characteristics of the wing with plain spoilers at low and moderate angles of attack. (See figs. 10 and 11.) At high angles of attack, however, the spoilers retained more of their effectiveness on the wing-fuselage combinations than on the wing alone.

Small projections of the plain or step spoilers gave reverse rolling moments such as have been previously noted for similarly located spoilers on unswept wings. (See reference 12.) Extending the step spoilers inboard from the tip caused increases in rolling moment which were less than proportional to the increases in spoiler span in the low and moderate angle-of-attack range. At angles of attack where stalling occurred on the wing the inboard portions of the spoiler were ineffective in producing rolling moments. The rolling moments for the plain spoiler were approximately proportional to the spoiler span at low and moderate angles of attack when the spoiler was extended from the tip to the  $0.60\frac{b}{2}$  station. Farther extension inboard to the  $0.35\frac{b}{2}$  station resulted in increased rolling moments but in a smaller proportion than was observed for the outboard spoilers. Extension inboard to the side of the fuselage resulted in no further increase in rolling moment even at low angles of attack where no stalling occurred. At high angles of attack the inboard portions of the spoiler lost their effectiveness to the extent that the spoiler on the outer 20 percent of the semispan produced as much rolling moment as the spoiler extending from the tip to the side of the fuselage. The outboard portions of the plain spoiler were slightly more effective than those of the step spoiler in the low and

moderate angle-of-attack range, but the step spoiler was more effective than the plain spoiler in the high angle-of-attack range.

Wing and fuselage with leading-edge and trailing-edge flaps.— The addition of 0.40-span leading-edge flaps (fig. 12) had practically no effect on the spoiler characteristics. The further addition of full-span double slotted flaps (fig. 13) caused a considerable increase in effectiveness for both the plain and step spoiler. Extending the spoiler inboard from the tip caused about the same percentage increases in rolling moment as were noted on the model without flaps.

Tests of inboard spoilers showed that at an angle of attack of  $1^{\circ}$  a 58-percent-semispan inboard plain spoiler produced less rolling moment than an 18-percent-semispan outboard spoiler. The inboard step spoiler was somewhat more effective than the inboard plain spoiler. At the same angle of attack the 58-percent-semispan inboard step spoiler produced only about three-fourths the rolling moment that a 40-percent outboard step spoiler produced. As the angle of attack was increased, the effectiveness of the inboard plain and step spoilers decreased until at about  $15^{\circ}$  angle of attack the effectiveness was essentially zero.

#### Comparison of Aileron and Spoiler

Although data were obtained for aileron deflections up to  $\pm 25^{\circ}$ , it is improbable that deflections greater than about  $\pm 15^{\circ}$  can be obtained with a conventional internal nose balance on the aileron on a thin wing such as was used in the present tests. The 0.10c projection of the spoiler is probably the maximum that could be obtained with a retractable arc-type spoiler. The following comparison between the aileron and spoilers, therefore, has been made on the basis of a maximum total aileron deflection of  $30^{\circ}$  and a maximum spoiler projection of 0.10c.

The comparison shows that for the flaps-neutral configuration (fig. 14(a)) at  $C_L = 0.1$  a step spoiler extending from  $0.35\frac{b}{2}$  to the tip and projected 0.10c produced about the same rolling moment as a total aileron deflection of  $16^{\circ}$ . The plain spoiler under the same conditions produced about the same rolling moment as a total aileron deflection of  $18^{\circ}$ . At high angles of attack with flaps neutral the plain spoiler produced about the same rolling moment as a total aileron deflection of  $12^{\circ}$  and the step spoiler produced about the same rolling moment as a total aileron deflection of  $20^{\circ}$ . A total aileron deflection of  $30^{\circ}$  at  $C_L = 0.1$  produced about 65 percent more rolling moment than that obtained with the most effective spoiler tested. These equivalent aileron deflections are based on the low-speed data presented in this paper and do not account for compressibility and wing-twist effects.

Comparisons of the aileron and spoiler on the flaps-deflected configuration (fig. 14(b)) are made herein at the same lift coefficient rather than the same angle of attack because the spoiler allowed the use of full-span flaps, whereas the aileron limited the span of the flaps. At a lift coefficient of 0.90 a plain spoiler projected 0.10c on the outer 63 percent of the semispan produced a rolling-moment coefficient of -0.053 and a step spoiler produced a rolling-moment coefficient of -0.048. At the same lift coefficient a total aileron deflection of 30° produced a rolling-moment coefficient of -0.035. At  $0.9C_{L_{max}}$  (a lift coefficient of 1.60 and an angle of attack of 11.3° with spoilers deflected) the same plain spoiler or step spoiler produced a rolling-moment coefficient of -0.042, and a total aileron deflection of 30° ( $C_L = 1.60$ ;  $\alpha = 15.3^\circ$  with ailerons deflected) produced a rolling-moment coefficient of -0.029. At the highest angle of attack tested, the spoiler effectiveness decreased to less than one-half that at the low angles of attack. The spoiler rolling-moment coefficients at  $C_{L_{max}}$  are equivalent to about 20° total aileron deflection.

Thus, it can be seen that the spoiler configurations tested were more effective than the aileron on the flaps-deflected configuration below  $0.9C_{L_{max}}$ , but at  $C_{L_{max}}$  the aileron is superior to the spoiler.

Projecting the spoilers caused a change in pitching-moment trim, the magnitude and direction of which were dependent on the span and the type of spoiler. Deflecting the ailerons in opposite directions would produce practically no change in trim.

The yawing moments due to aileron deflection and rolling would produce sideslip in a direction which, due to the negative effective dihedral associated with sweepforward, would produce a rolling moment in the same direction as that due to the aileron deflection. Thus, on a wing such as the one tested the so-called "adverse" yawing moments due to aileron deflection and rolling would tend to increase the rolling moment and the "favorable" yawing moments due to spoiler projection would tend to decrease the rolling moment. An airplane design, however, would probably incorporate positive geometric dihedral to counteract the negative effective dihedral of the sweepforward with the result that adverse yawing moments would tend to reduce, and favorable yawing moments would tend to increase the rolling moments.

Values of the wing-tip helix angle in a roll  $\frac{pb}{2V}$  have been calculated for the spoilers and aileron on the high-speed and landing configurations of the wing. They were calculated from the relation

$$\frac{pb}{2V} = \frac{C_l}{C_{l_p}}$$

A value for  $C_{l_p}$  (wing damping coefficient in roll) was found to be -0.363 from the data of reference 11.

The calculations indicate that at  $C_L = 0.1$  with flaps neutral, a total aileron deflection of  $30^\circ$  will produce a value of  $\frac{pb}{2V}$  of about 0.10, and a plain step spoiler projected 0.10c on the outer 65 percent of the semispan will produce a value of  $\frac{pb}{2V}$  of about 0.06. As the angle of attack is increased, the value of  $\frac{pb}{2V}$ , which  $30^\circ$  total aileron deflection will produce, decreases until at  $0.9C_{L_{max}}$  ( $C_L = 1.04$ ) it is about 0.07. The value of  $\frac{pb}{2V}$ , which the spoiler will produce, increases as the angle of attack is increased to  $8^\circ$  so that at that angle either spoiler will produce a value of  $\frac{pb}{2V}$  of about 0.065. Above  $\alpha = 8^\circ$  the value of  $\frac{pb}{2V}$  decreases until, at  $0.9C_{L_{max}}$ , it is about 0.04 for the plain spoiler and about 0.03 for the step spoiler.

The calculations for the flap-deflected configuration indicated that at low angles of attack ( $C_L = 0.8$ ) a total aileron deflection of  $30^\circ$  will produce a value of  $\frac{pb}{2V}$  of about 0.10, the step spoiler about 0.13, and the plain spoiler about 0.15. At  $0.9C_{L_{max}}$  ( $C_L = 1.6$ ) the aileron will produce a value of  $\frac{pb}{2V}$  of about 0.08 and either spoiler will produce about 0.12.

A total aileron deflection of  $30^\circ$  will produce values of  $\frac{pb}{2V}$  which satisfy the requirements of the Army and Navy stability and control specifications (references 13 and 14) on both the flaps-neutral and flaps-deflected configurations.

Values of  $\frac{pb}{2V}$  which the spoilers will produce are larger than required for the flaps-deflected configuration but smaller than required for the flaps-neutral configuration. Allowances have not been made in the calculations for the effects of compressibility and wing twist on the flaps-neutral configuration or the effects of sideslip on the flaps-deflected configuration. Unpublished data indicate that compressibility effects increase spoiler effectiveness and decrease aileron effectiveness. Thus, it is possible that the spoilers would produce satisfactory values of  $\frac{pb}{2V}$  at high speeds. The  $\frac{pb}{2V}$  values obtainable with the spoilers on the flap-neutral configuration at high angles of attack, however, are considerably below the specification requirements.

### CONCLUSIONS

A lateral-control investigation at a Reynolds number of 5,300,000 of a 32° sweptforward wing of aspect ratio 5.8 indicated the following conclusions:

1. The rate of change of rolling-moment coefficient with aileron deflection  $C_{l\delta}$  decreased from about 0.00115 at low angles of attack to about 0.00060 at maximum lift. The value of  $C_{l\delta}$  for low angles of attack was predicted with reasonable accuracy.
2. The addition of a leading-edge flap on the inboard portion of the wing resulted in a slight increase in  $C_{l\delta}$  through most of the angle-of-attack range but had a negligible effect at maximum lift. When a partial-span double slotted flap was deflected in combination with the leading-edge flap,  $C_{l\delta}$  did not decrease to as low a value at maximum lift as with flaps neutral.
3. The yawing-moment characteristics of the aileron were similar to those for straight wings; that is, ailerons deflected for a roll to the right produced yawing moments tending to yaw the model to the left.
4. The rate of change of hinge-moment coefficient with deflection  $C_{h\delta}$  for the unbalanced aileron increased from -0.0062 at low angles of attack to -0.0094 at maximum lift. The rate of change of hinge-moment coefficient with angle of attack  $C_{h\alpha}$  for the unbalanced aileron increased from -0.0046 at low angles of attack to about -0.0175 at maximum lift.

5. The leading-edge flap had a negligible effect on the aileron hinge-moment characteristics. The combination of leading-edge and double slotted flaps, however, caused an increase in  $C_{h\delta}$  through the angle-of-attack range and a large decrease in  $C_{h\alpha}$  in the high angle-of-attack range.

6. Calculations which combined the effects of  $C_{h\alpha}$  and an internal nose balance on  $C_{h\delta}$  in steady rolling indicate that, if the aileron is balanced for the high-speed condition, the underbalance which would occur at high angles of attack might produce excessive control stick forces in the low-speed conditions.

7. Spoiler lateral controls located on the inboard portion of the wing were considerably less effective in producing rolling moments than spoilers located near the tips even at low angles of attack where there was no stalling on the wing. A spoiler on the outboard 20 percent of the semispan maintained most of its effectiveness to the highest angle of attack tested. The rolling effectiveness was about the same for a step spoiler as for a plain spoiler.

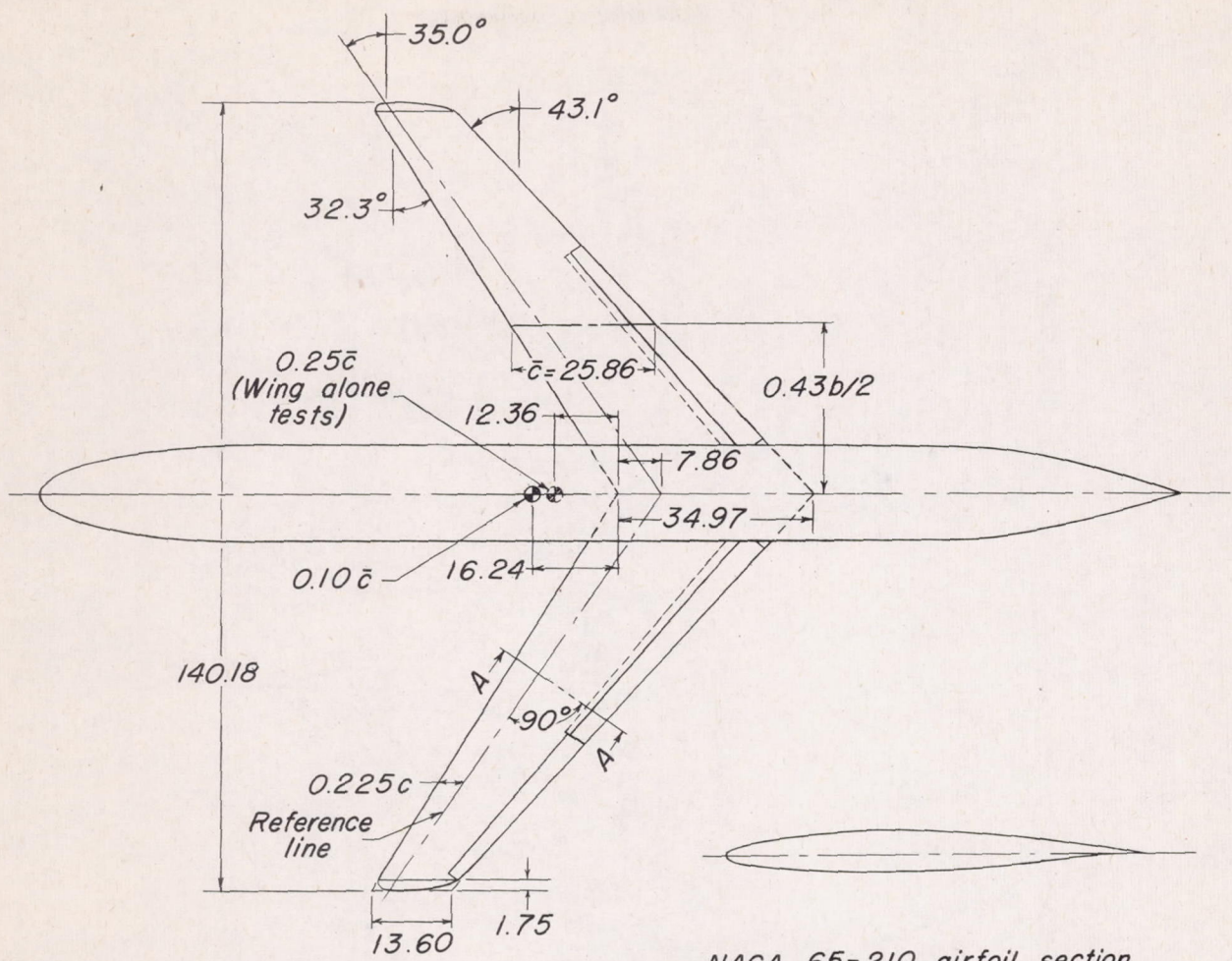
8. The maximum rolling moment due to projecting the spoiler 10 percent of the wing chord was equivalent to about 20° total aileron deflection for the flap-neutral configuration. The same spoiler on the wing with full-span double slotted flaps and an inboard leading-edge flap produced about the same rolling moments at all lift coefficients below  $0.9C_{L_{max}}$  as 50° total aileron deflection produced on the wing with partial-span double slotted flaps and the leading-edge flap. Above  $0.9C_{L_{max}}$ , however, the effectiveness of the spoilers decreased sharply.

Langley Aeronautical Laboratory  
National Advisory Committee for Aeronautics  
Langley Air Force Base, Va.

## REFERENCES

1. Graham, Robert R., and Conner, D. William: Investigation of High-Lift and Stall-Control Devices on an NACA 64-Series 42° Sweptback Wing with and without Fuselage. NACA RM L7G09, 1947.
2. Koven, William, and Graham, Robert R.: Wind-Tunnel Investigation of High-Lift and Stall-Control Devices on a 37° Sweptback Wing of Aspect Ratio 6 at High Reynolds Numbers. NACA RM L8D29, 1948.
3. Graham, Robert R., and Koven, William: Lateral-Control Investigation on a 37° Sweptback Wing of Aspect Ratio 6 at a Reynolds Number of 6,800,000. NACA RM L8K12, 1949.
4. Martina, Albert P., and Deters, Owen J.: Maximum Lift and Longitudinal Stability Characteristics at Reynolds Numbers up to  $7.8 \times 10^6$  of a 32° Sweptforward Wing Equipped with High-Lift and Stall-Control Devices, Fuselage, and Horizontal Tail. NACA RM L9H18a, 1949.
5. Sivells, James C., and Spooner, Stanley H.: Investigation in the Langley 19-Foot Pressure Tunnel of Two Wings of NACA 65-210 and 64-210 Airfoil Sections with Various Type Flaps. NACA TN 1579, 1948.
6. Eisenstadt, Bertram J.: Boundary-Induced Upwash for Yawed and Swept-Back Wings in Closed Circular Wind Tunnels. NACA TN 1625, 1948.
7. Bird, J. D.: Effect of Leakage past Aileron Nose on Aerodynamic Characteristics of Plain and Internally Balanced Ailerons on NACA 66(215)-216,  $a = 1.0$  Airfoil. NACA ACR L5F13a, 1945.
8. Lowry, John G., and Schneiter, Leslie E.: Estimation of Effectiveness of Flap-Type Controls on Sweptback Wings. NACA TN 1674, 1948.
9. Toll, Thomas A., and Schneiter, Leslie E.: Approximate Relations for Hinge-Moment Parameters of Control Surfaces on Swept Wings at Low Mach Numbers. NACA TN 1711, 1948.
10. Langley Research Staff (Compiled by Thomas A. Toll): Summary of Lateral-Control Research. NACA Rep. 868, 1947.
11. Bird, John D.: Some Theoretical Low-Speed Span Loading Characteristics of Swept Wings in Roll and Sideslip. NACA TN 1839, 1949.

12. Fischel, Jack, and Tamburello, Vito: Investigation of Effect of Span, Spanwise Location, and Chordwise Location of Spoilers on Lateral Control Characteristics of a Tapered Wing. NACA TN 1294, 1947.
13. Anon.: Stability and Control Characteristics of Airplanes. AAF Specification No. R-1815-A, April 7, 1945.
14. Anon.: Specification for Stability and Control Characteristics of Airplanes. SR-119A, Bur. Aero., April 7, 1945.



Section A-A

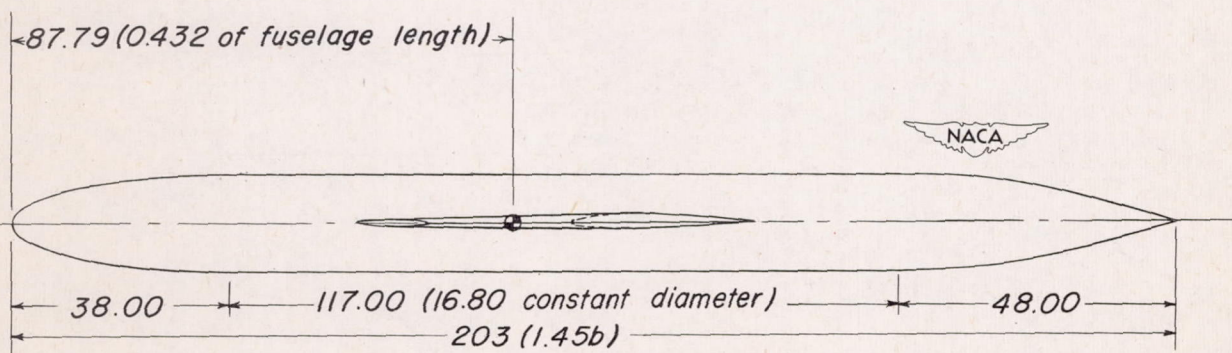


Figure 1.- Details of wing and fuselage.  $A = 5.79$ ;  $S = 23.58$  sq ft; taper ratio = 0.389; washout =  $1.8^\circ$ ; dihedral at reference line =  $0^\circ$ ; incidence at root chord =  $0^\circ$ ; fuselage fineness ratio = 12:1. Linear dimensions in inches unless noted.

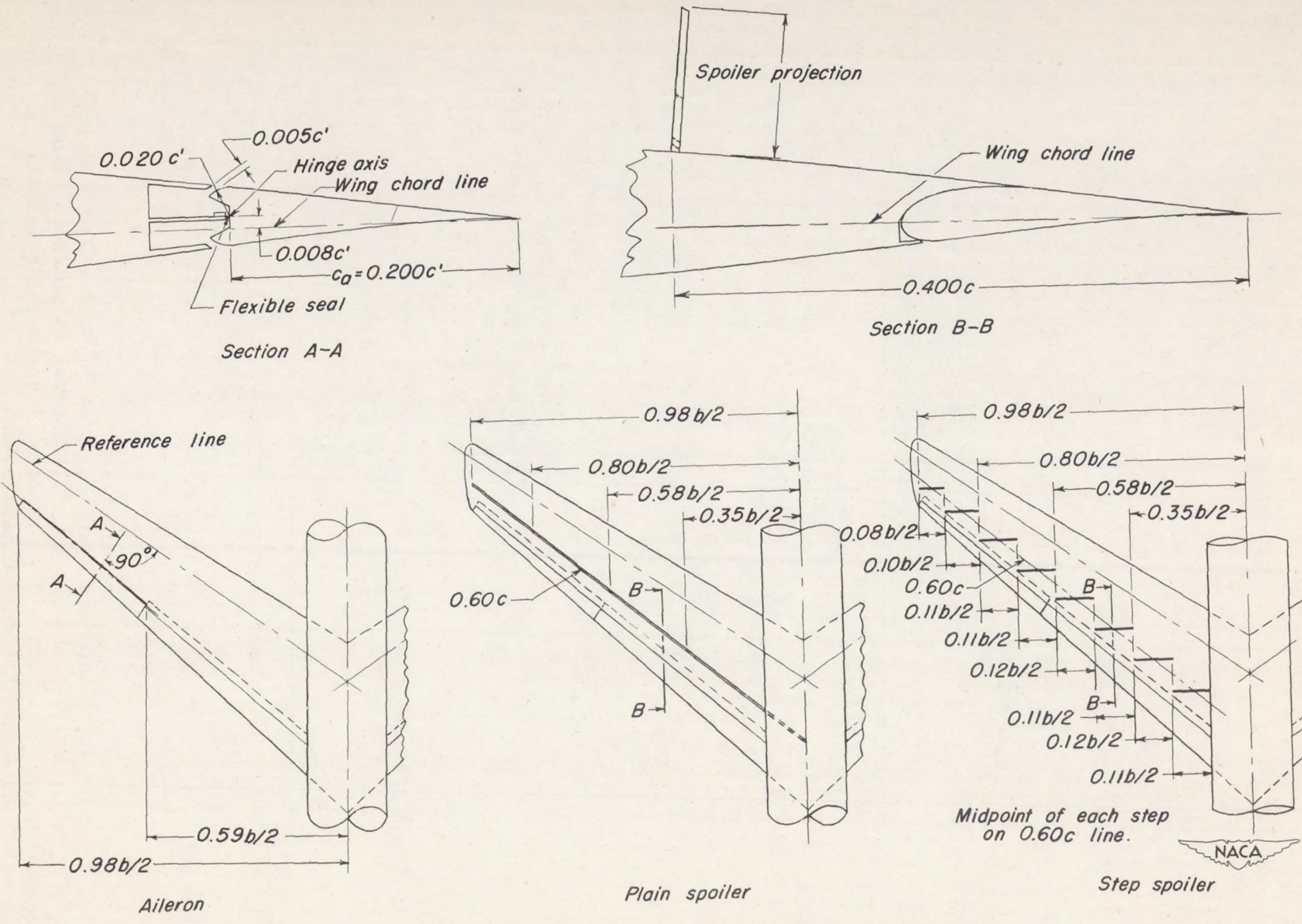


Figure 2.- Details of lateral-control devices.

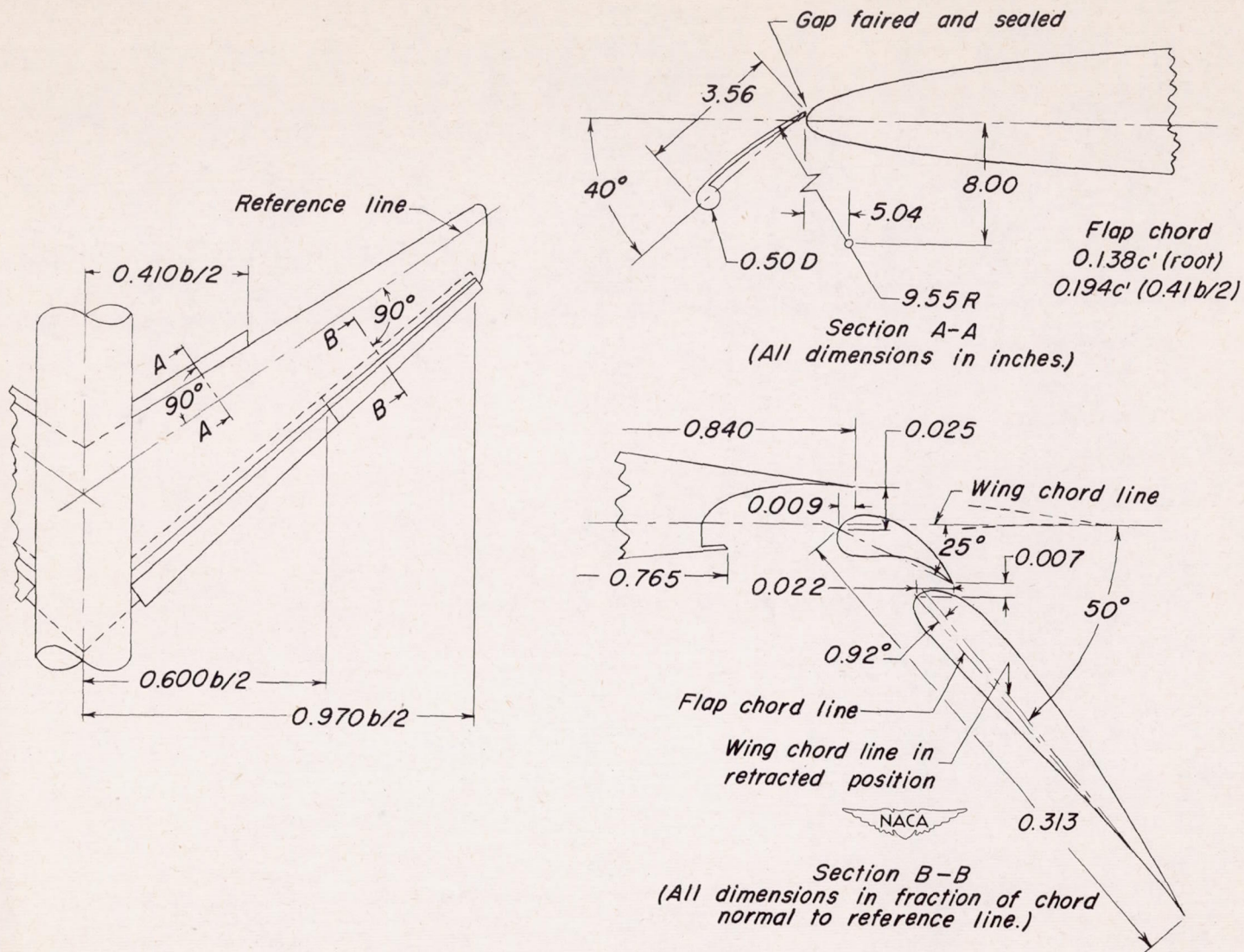


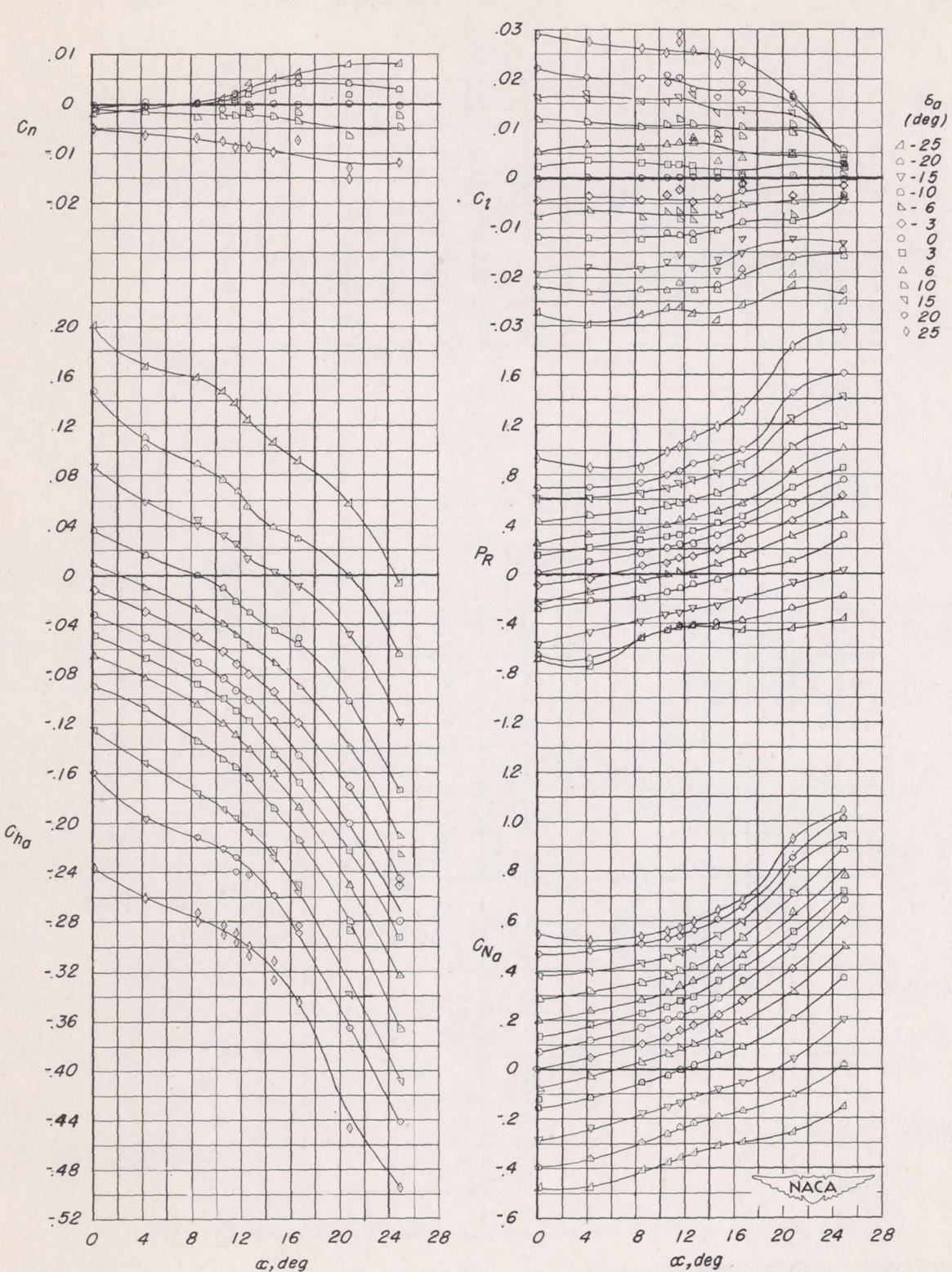
Figure 3.- Details of leading-edge and trailing-edge flaps.





Figure 4.- The  $32^\circ$  sweptforward wing with fuselage and leading-edge flap mounted in the Langley 19-foot pressure tunnel.



(a)  $C_l$ ,  $C_n$ ,  $C_{h_a}$ ,  $C_{N_a}$ , and  $P_R$  against  $\alpha$ .Figure 5.- Aileron characteristics on a  $32^\circ$  sweptforward wing with fuselage.

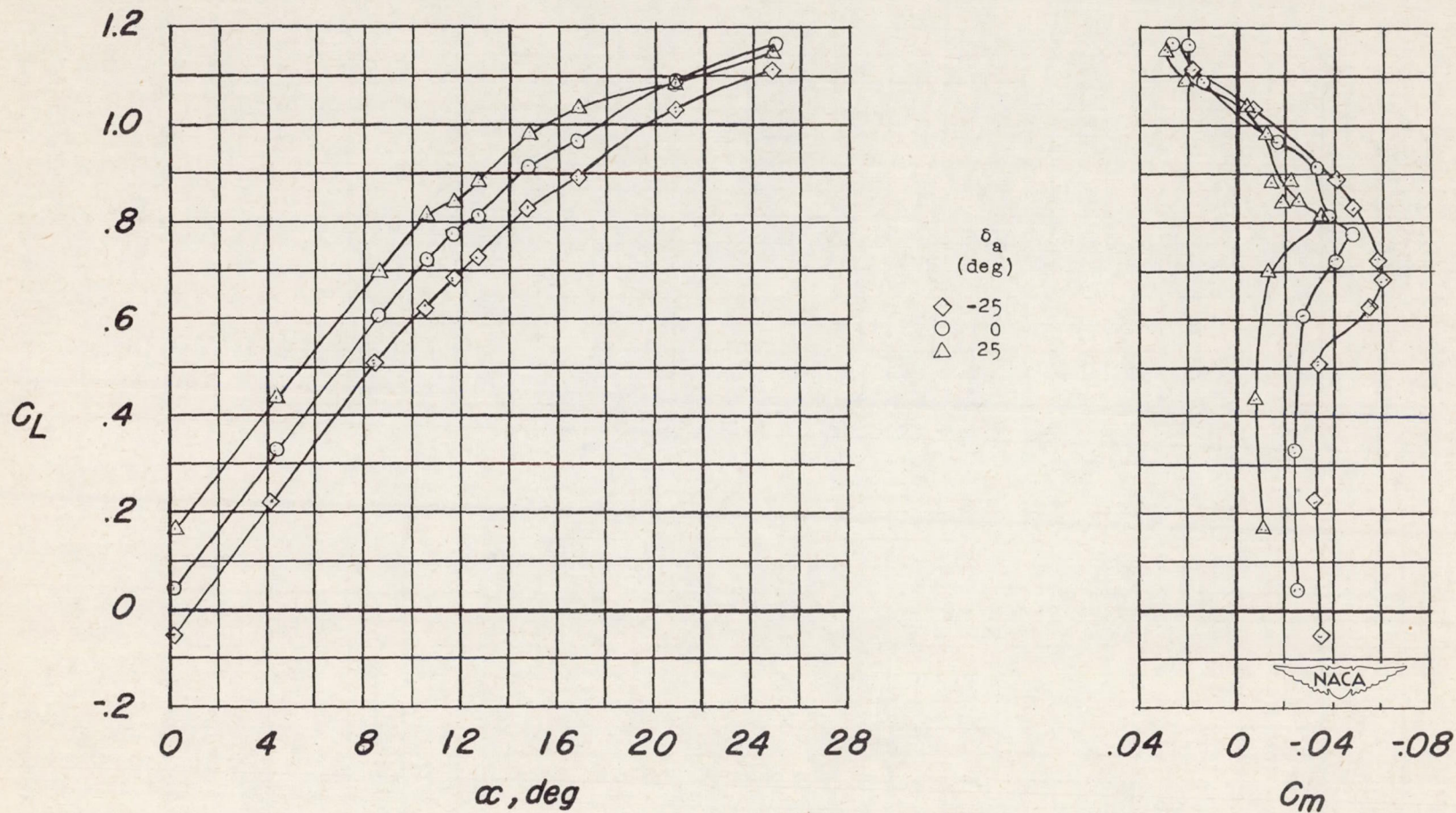
(b)  $C_L$  against  $\alpha$  and  $C_m$ .

Figure 5.- Concluded.

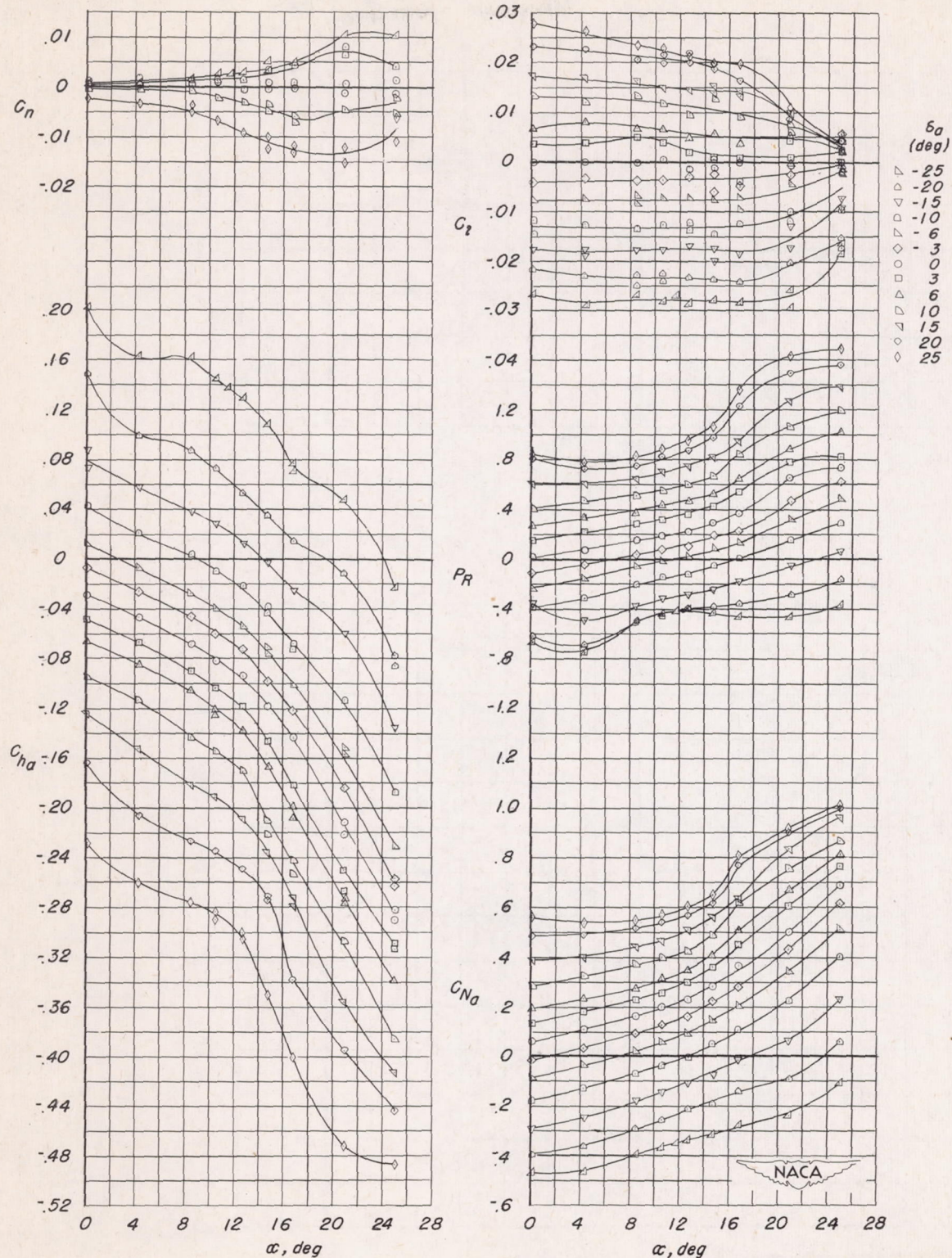
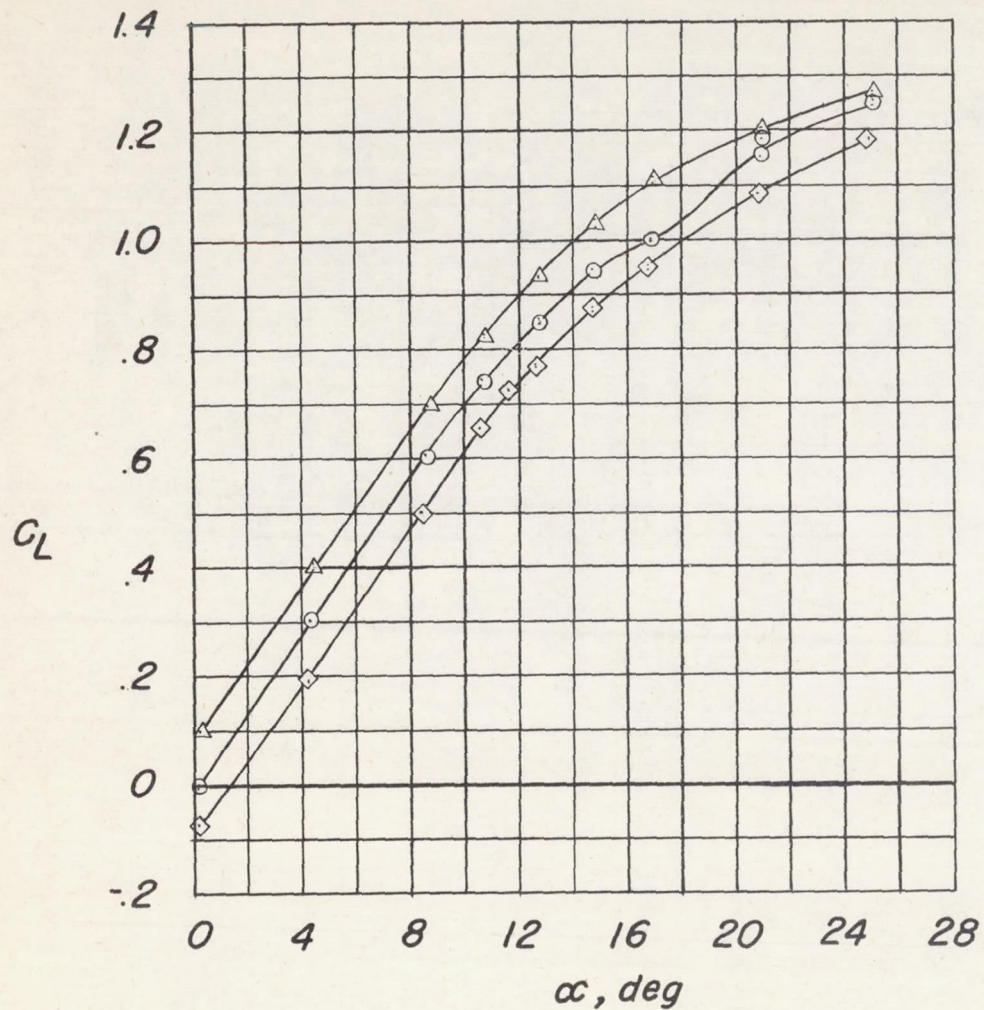
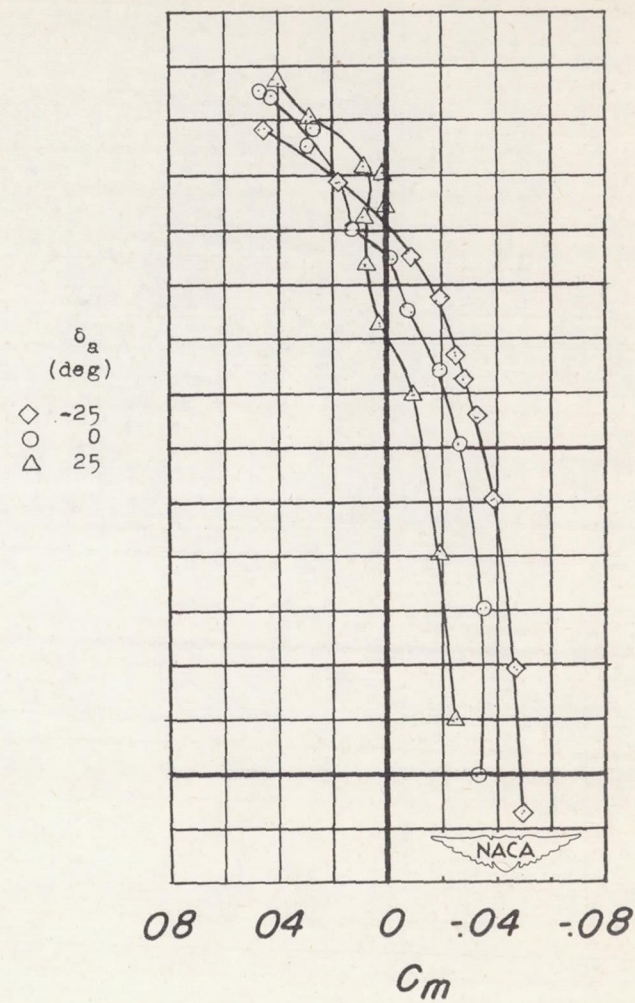
(a)  $C_l$ ,  $C_n$ ,  $C_{h\alpha}$ ,  $C_{N\alpha}$ , and  $P_R$  against  $\alpha$ .

Figure 6.- Aileron characteristics on a  $32^\circ$  sweptforward wing with fuselage and leading-edge flap.



(b)  $C_L$  against  $\alpha$  and  $C_m$ .

Figure 6.- Concluded.



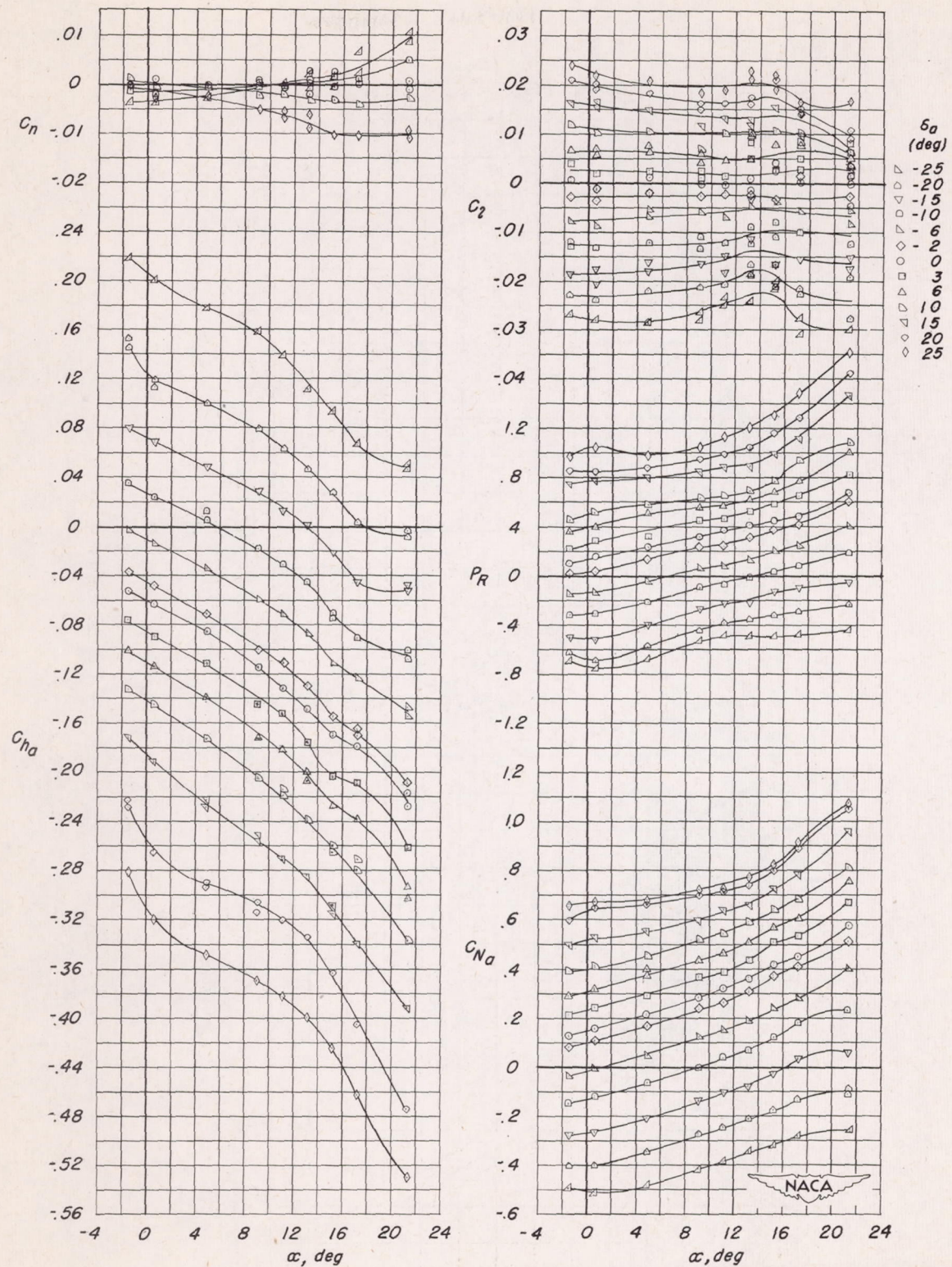
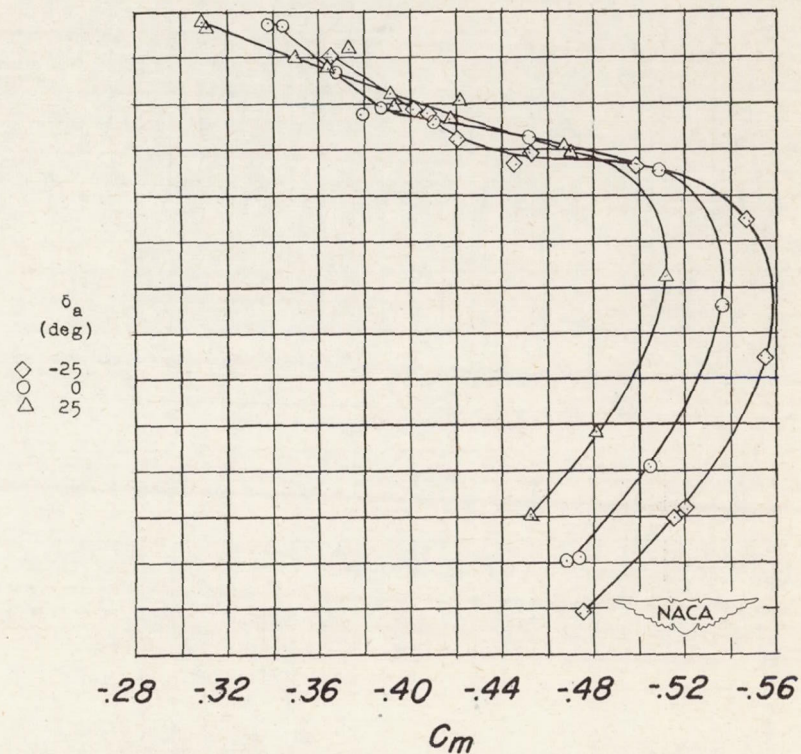
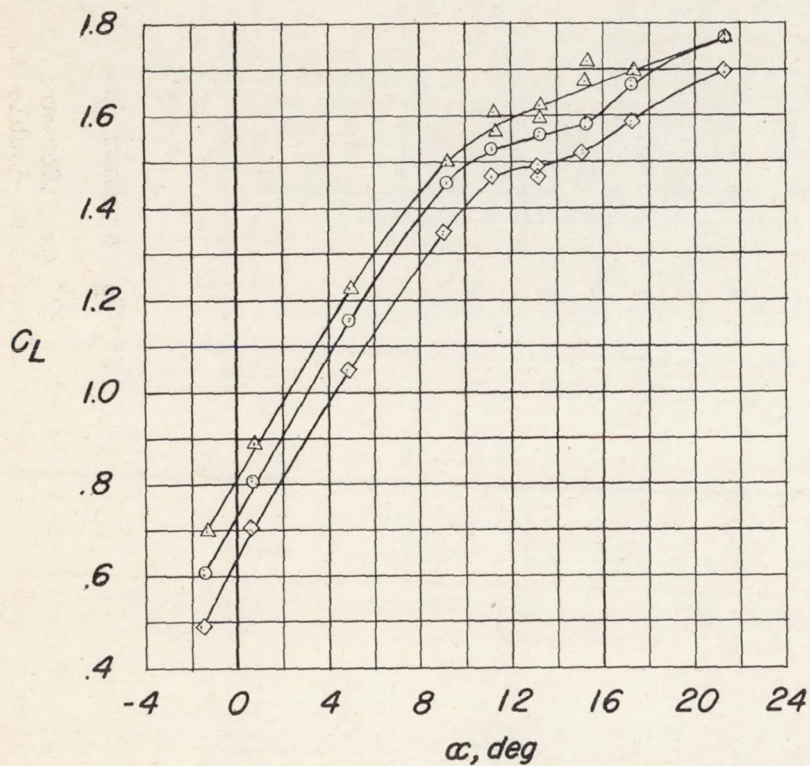
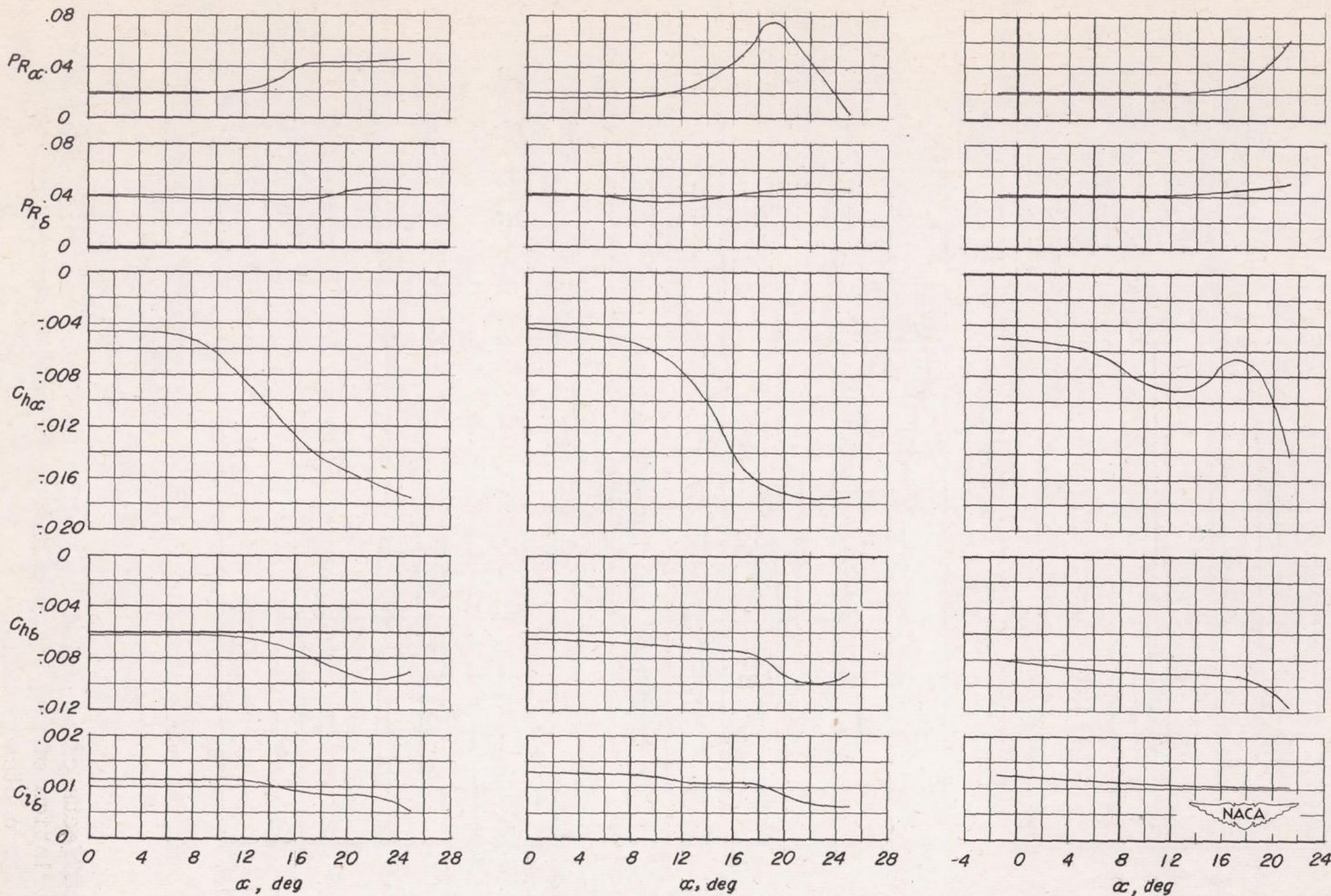
(a)  $C_l$ ,  $C_n$ ,  $C_{Na}$ , and  $P_R$  against  $\alpha$ .

Figure 7.- Aileron characteristics on a 32° sweptforward wing with fuselage, leading-edge flap, and partial-span double slotted flap.



(b)  $C_L$  against  $\alpha$  and  $C_m$ .

Figure 7.- Concluded.



(a) Flaps neutral. (b) Leading-edge flap deflected. (c) Leading-edge flap and double slotted flap deflected.

Figure 8.- Variation of aileron control and hinge-moment parameters with angle of attack of  $32^\circ$  swept-forward wing with fuselage.  $\delta_a = 0^\circ$ .

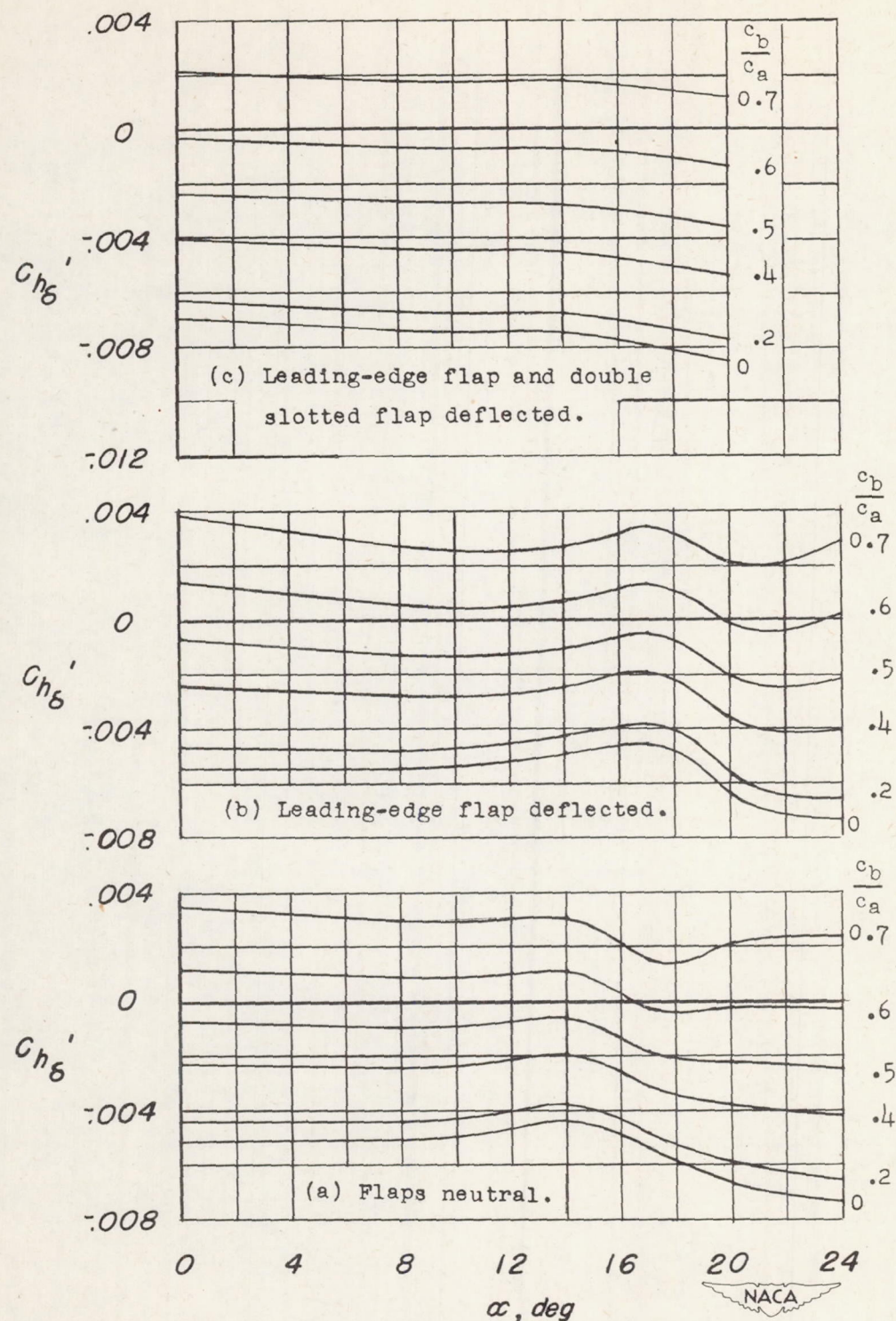
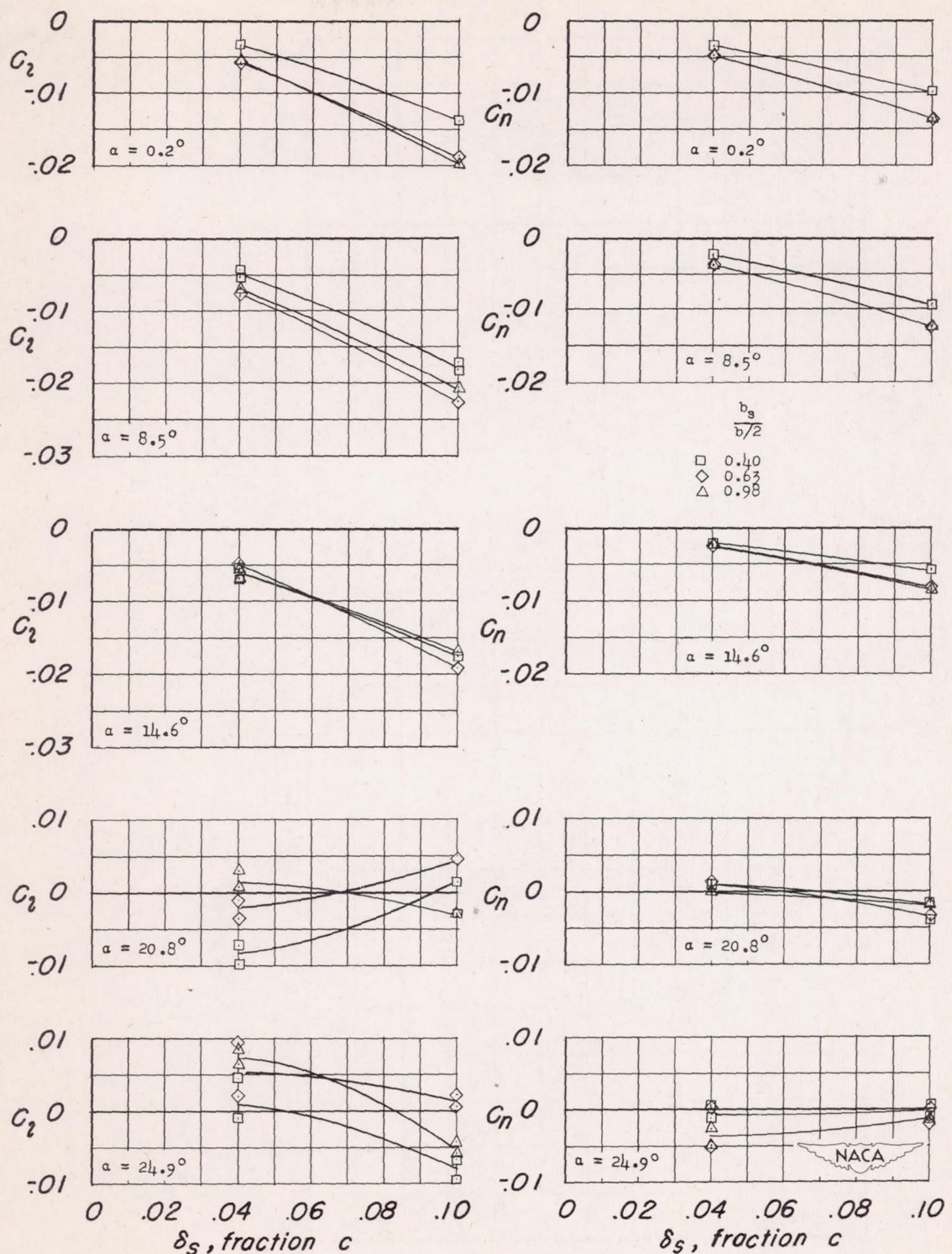
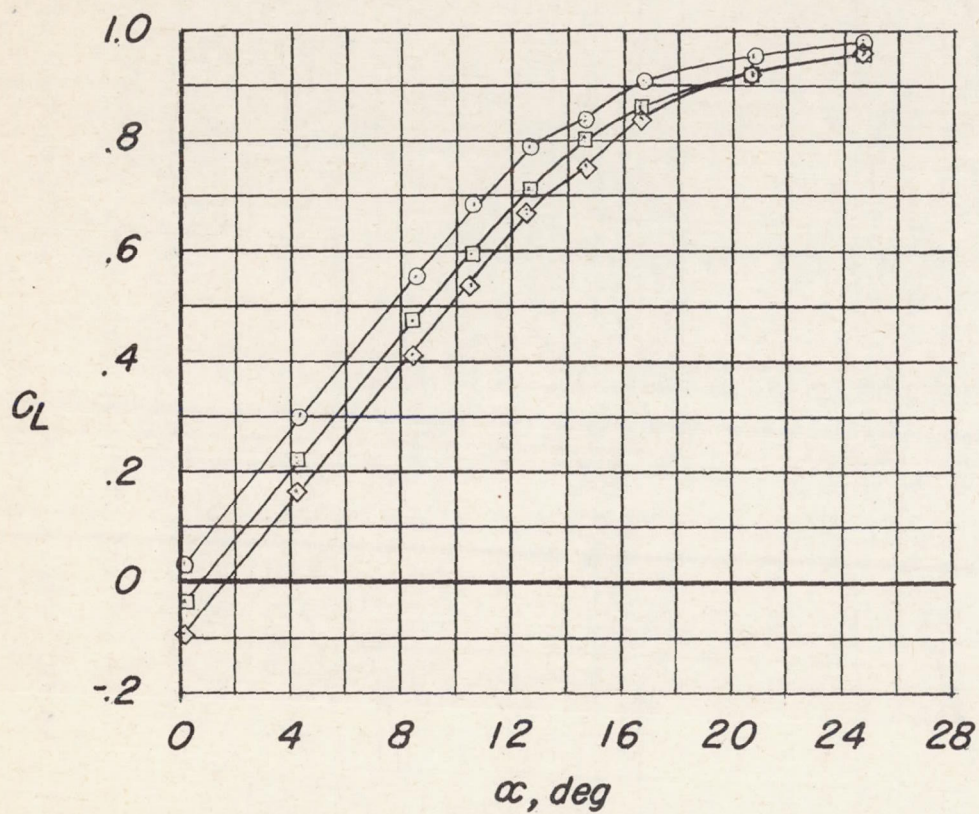


Figure 9.- Effects of a sealed internal balance on the hinge-moment characteristics of the aileron on the  $32^\circ$  sweptforward wing with fuselage in a steady roll.

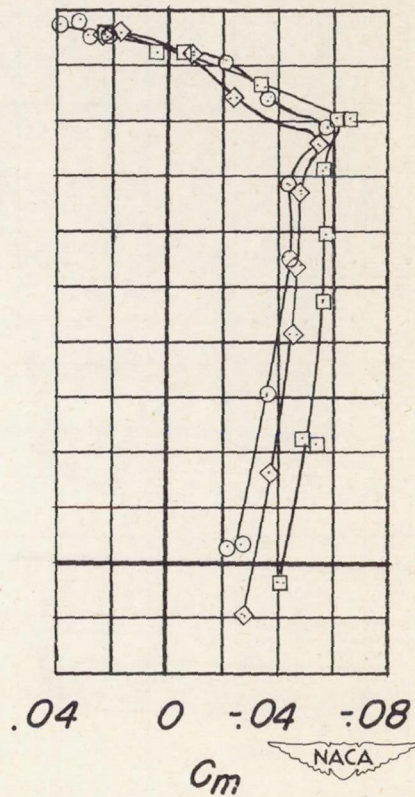


(a) Rolling and yawing moments.

Figure 10.- Characteristics of an outboard plain spoiler on a  $32^\circ$  sweptforward wing.

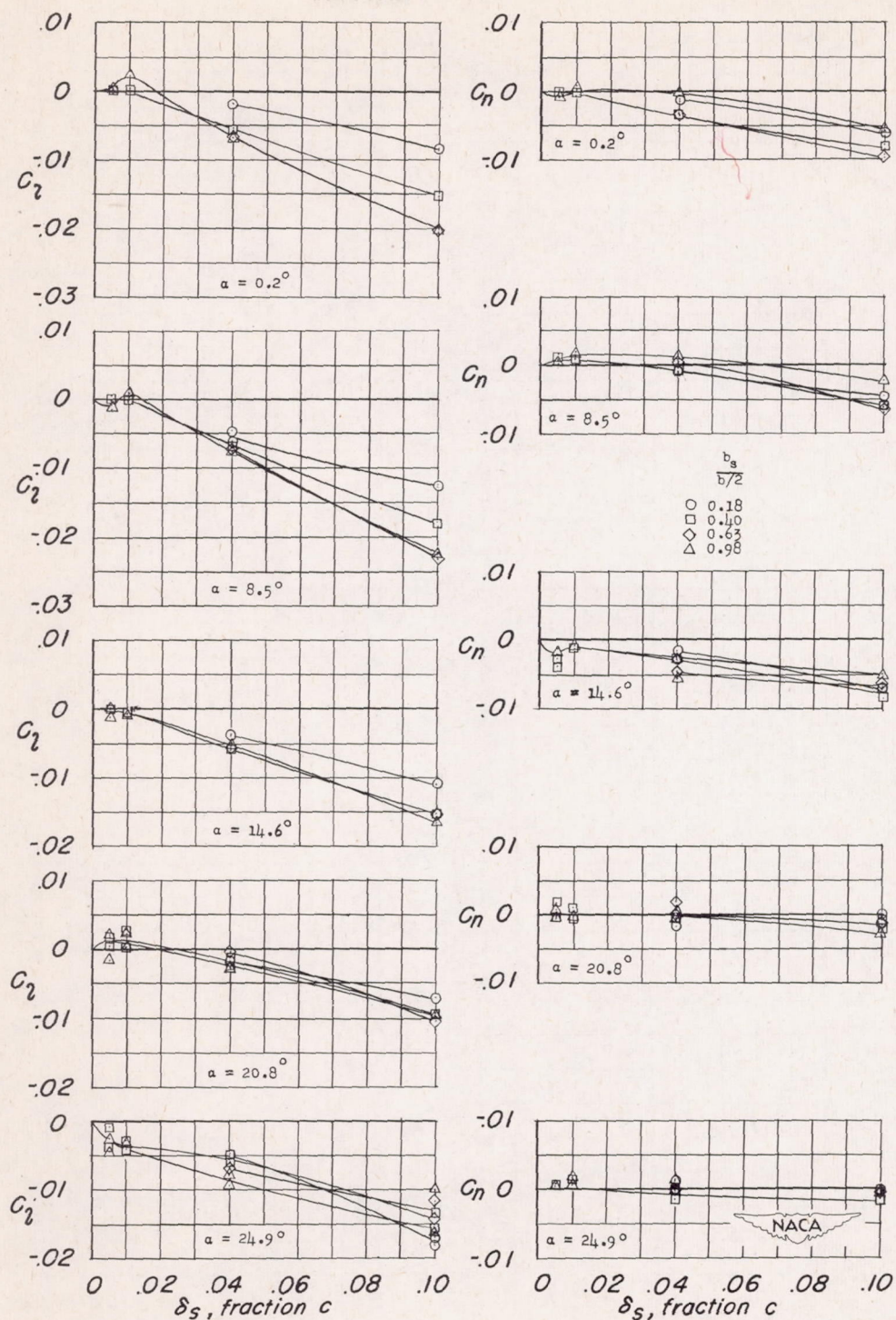


$\frac{b_s}{b/2}$   
 0  
 0.40  
 0.63



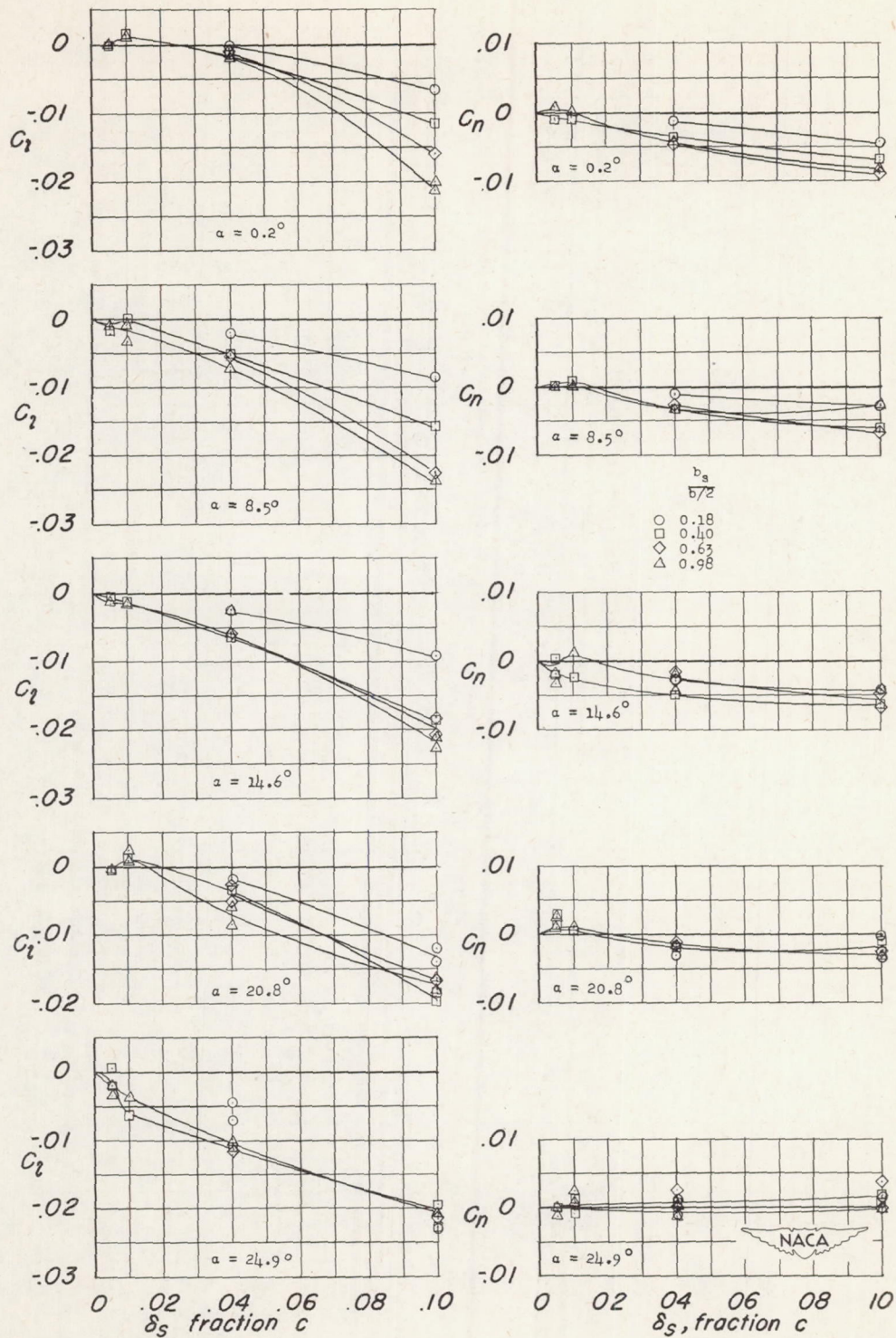
(b) Lift and pitching moment;  $\delta_s = 0.10c$ .

Figure 10.- Concluded.



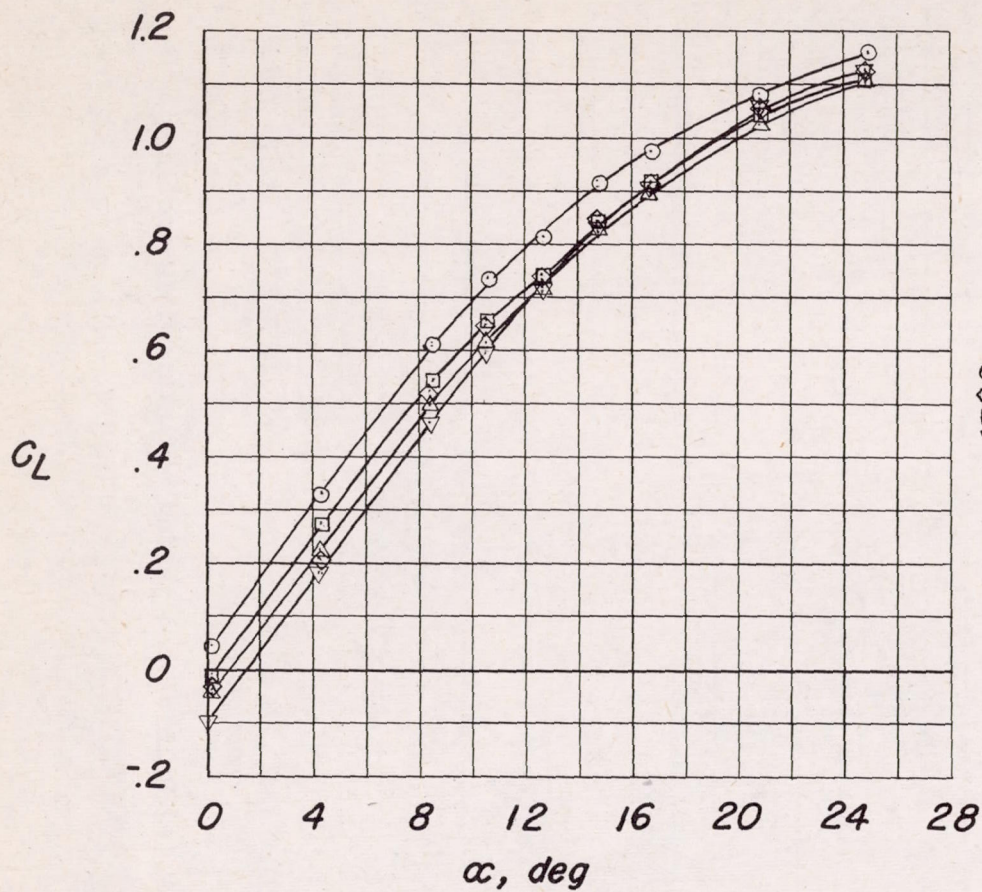
(a) Rolling and yawing moments; plain spoiler.

Figure 11.- Characteristics of outboard spoilers on a  $32^\circ$  sweptforward wing with fuselage.

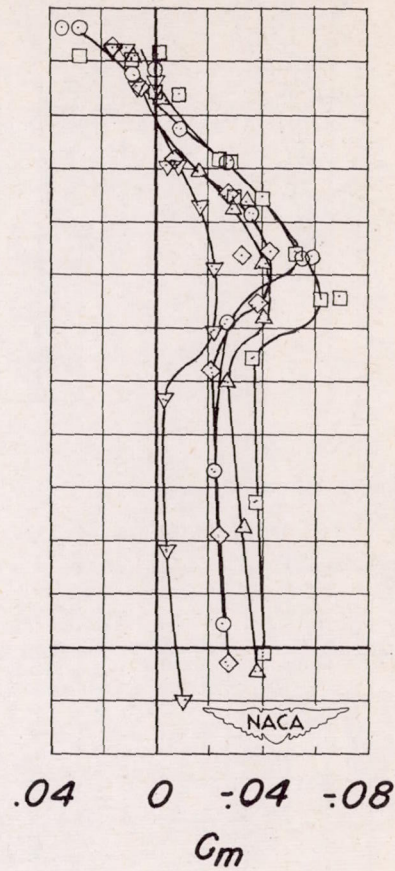


(b) Rolling and yawing moments; step spoiler.

Figure 11.- Continued.

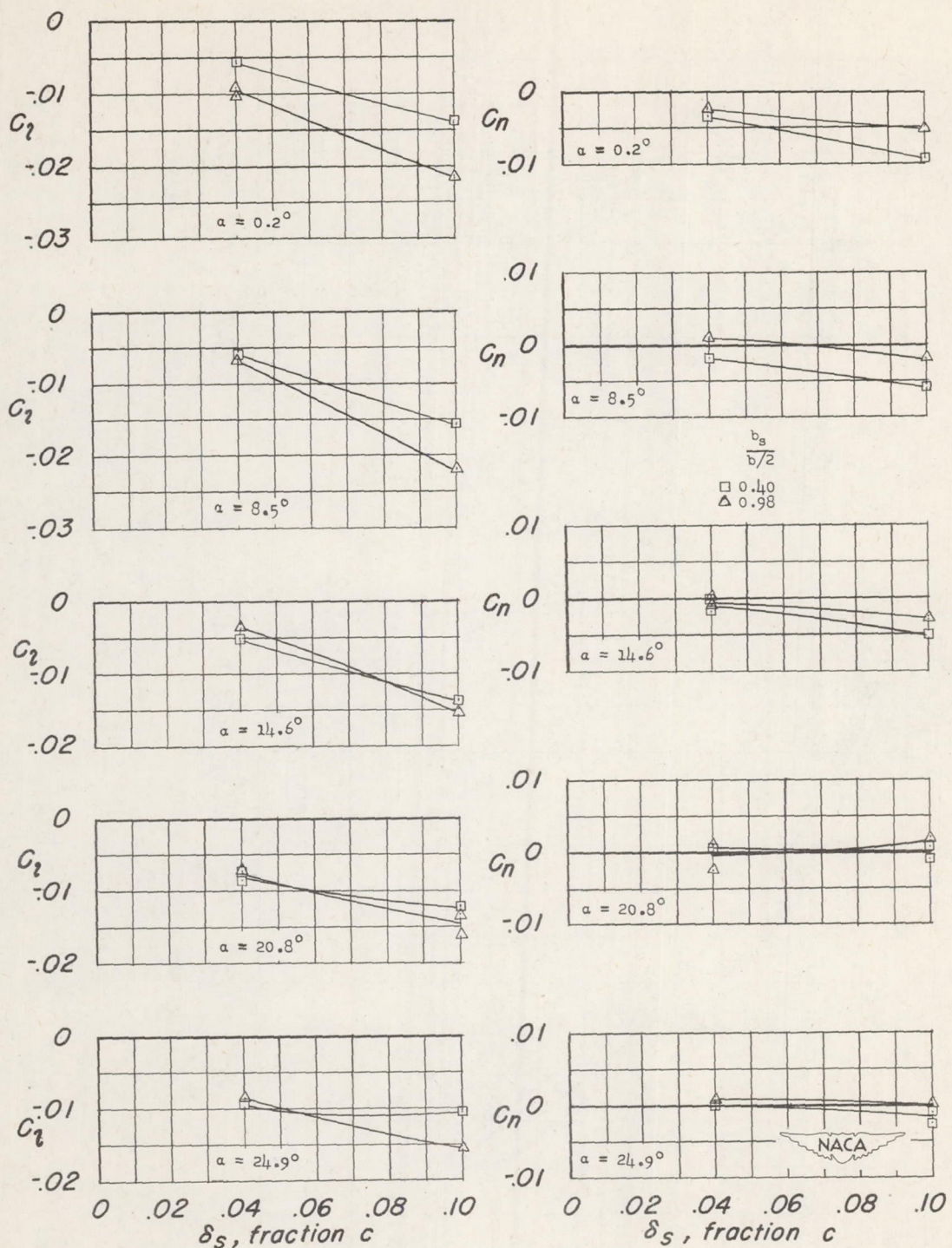


$b_s/b/2$	Spoiler type
0	○
0.40	◇
0.40	□
0.63	▽
0.63	△



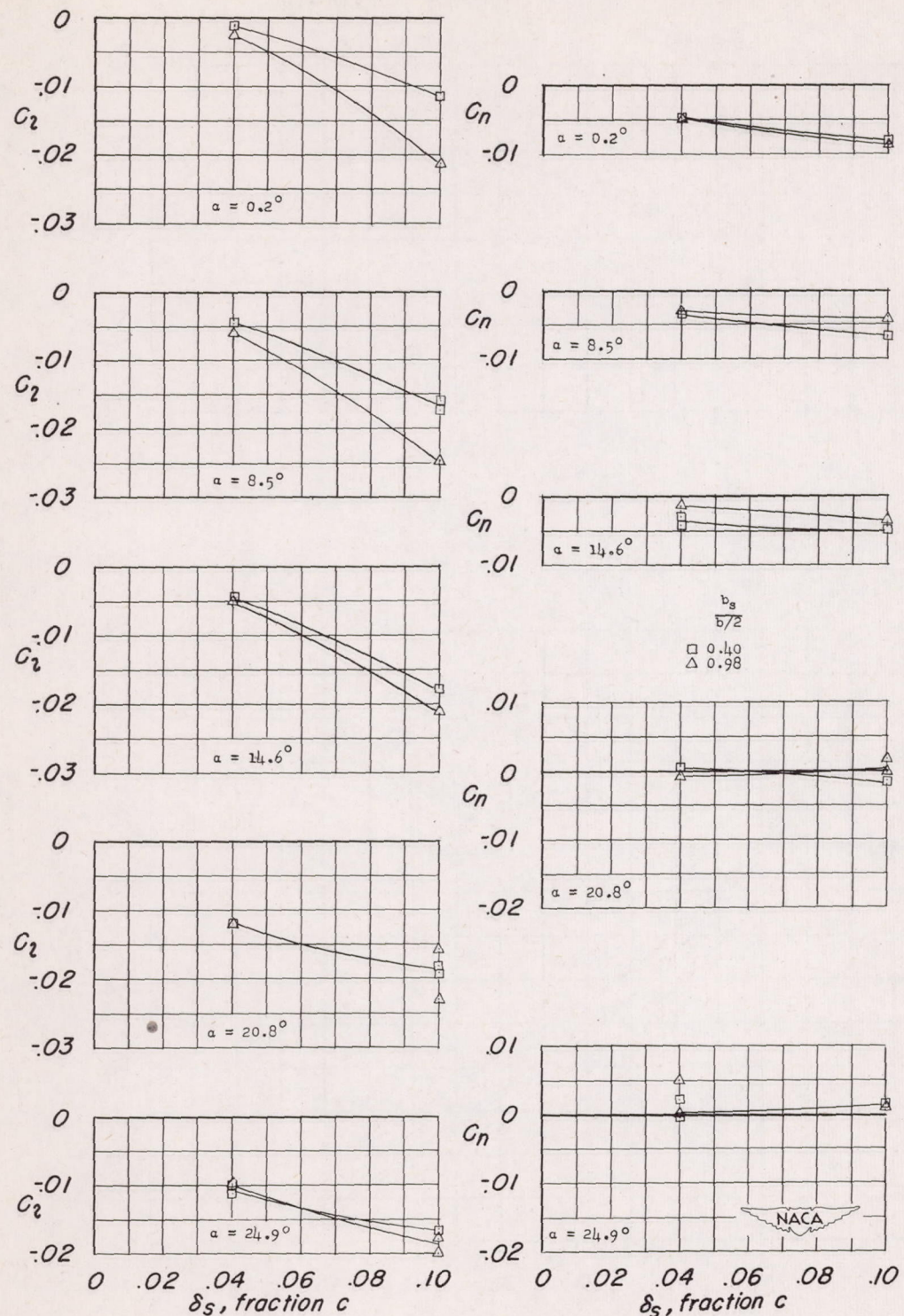
(c) Lift and pitching moment;  $\delta_s = 0.10c$ .

Figure 11.- Concluded.



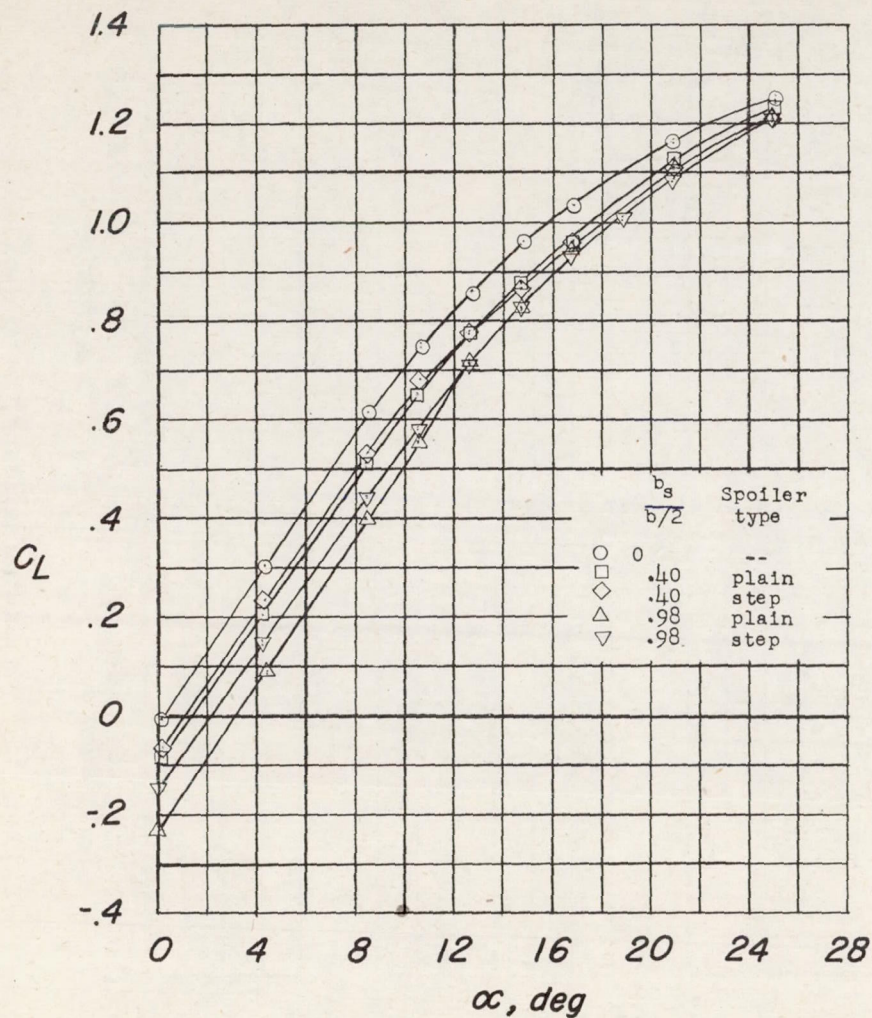
(a) Rolling and yawing moments; plain spoiler.

Figure 12.- Characteristics of outboard spoilers on a  $32^\circ$  sweptback wing with fuselage and leading-edge flaps.



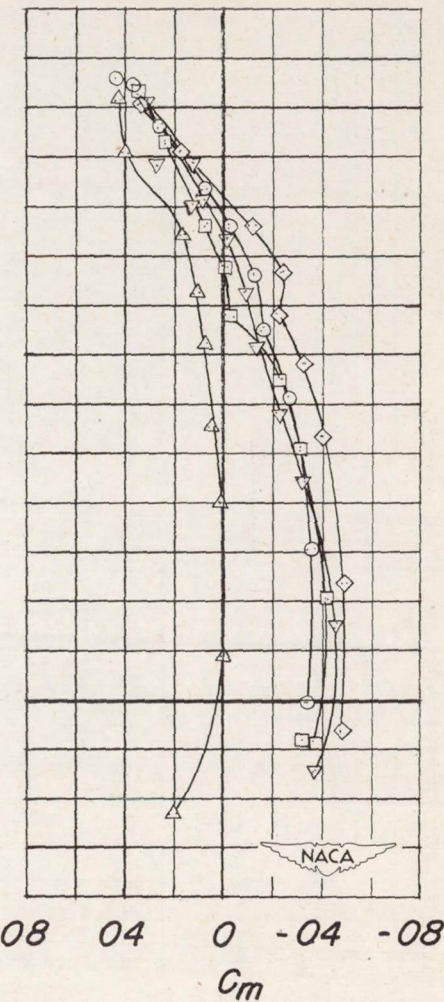
(b) Rolling and yawing moments; step spoiler.

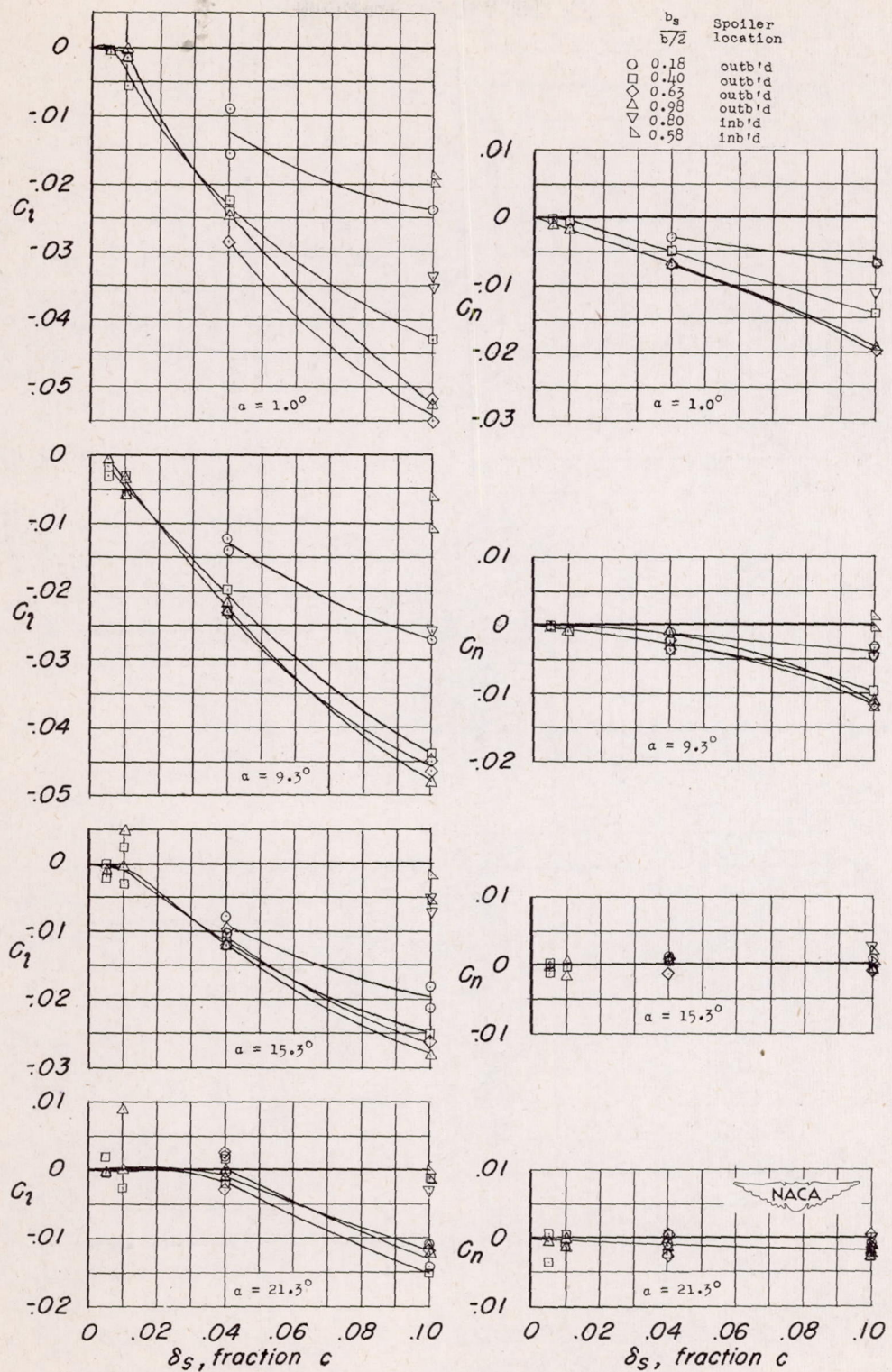
Figure 12.- Continued.



(c) Lift and pitching moment;  $\delta_s = 0.10c$ .

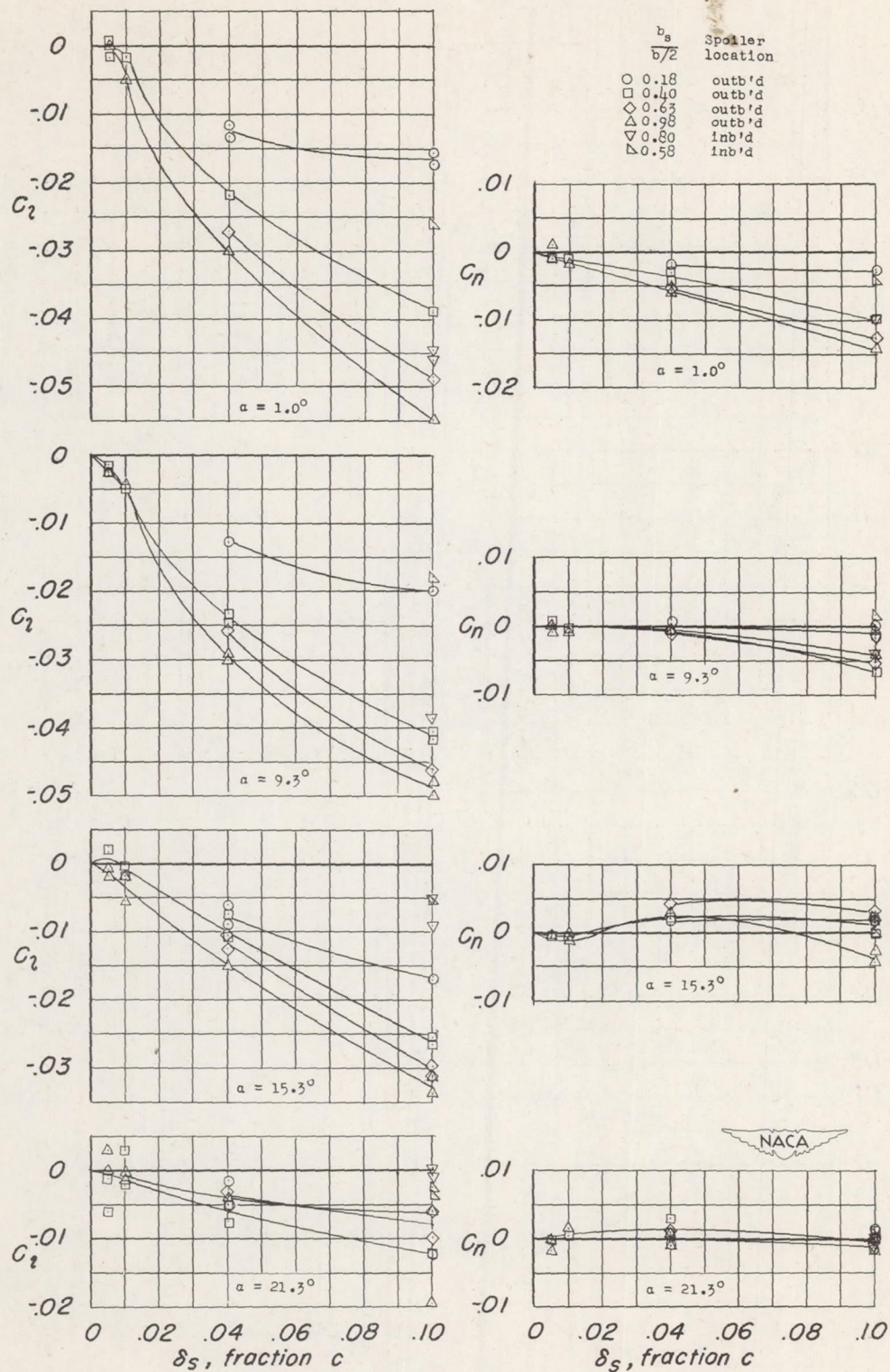
Figure 12.-- Concluded.





(a) Rolling and yawing moments; plain spoilers.

Figure 13.- Characteristics of spoilers on a 32° sweptforward wing with fuselage, leading-edge flap, and double slotted flap.



(b) Rolling and yawing moments; step spoiler.

Figure 13.- Continued.

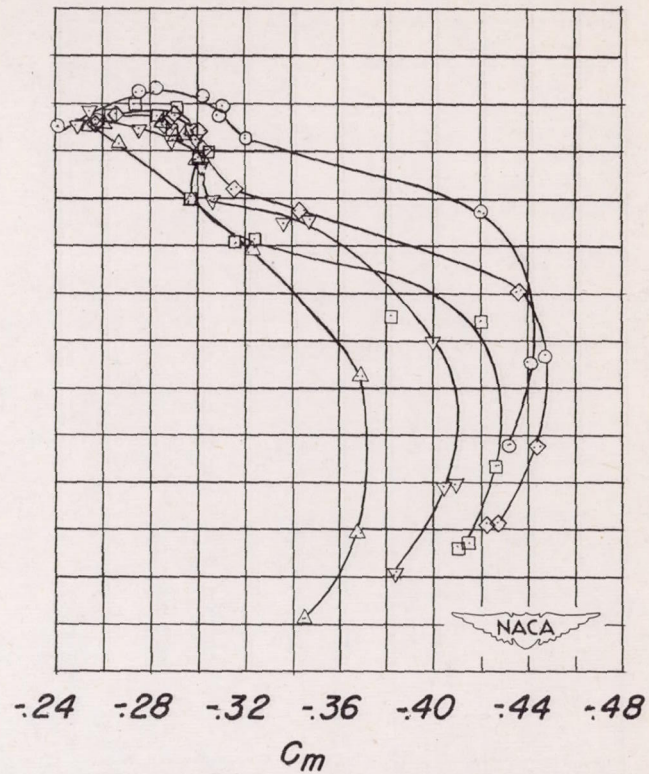
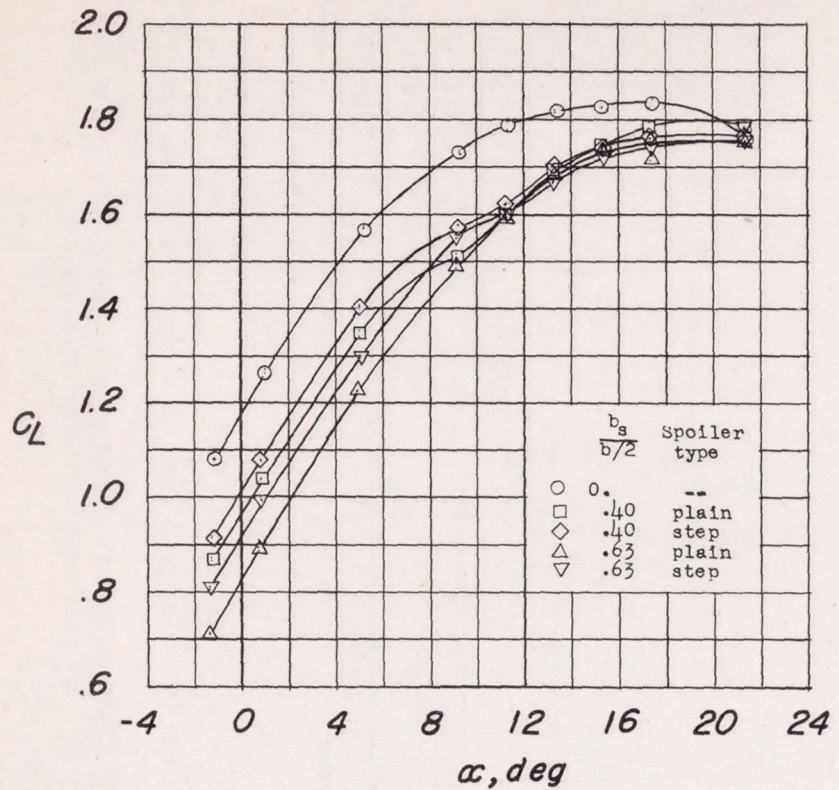
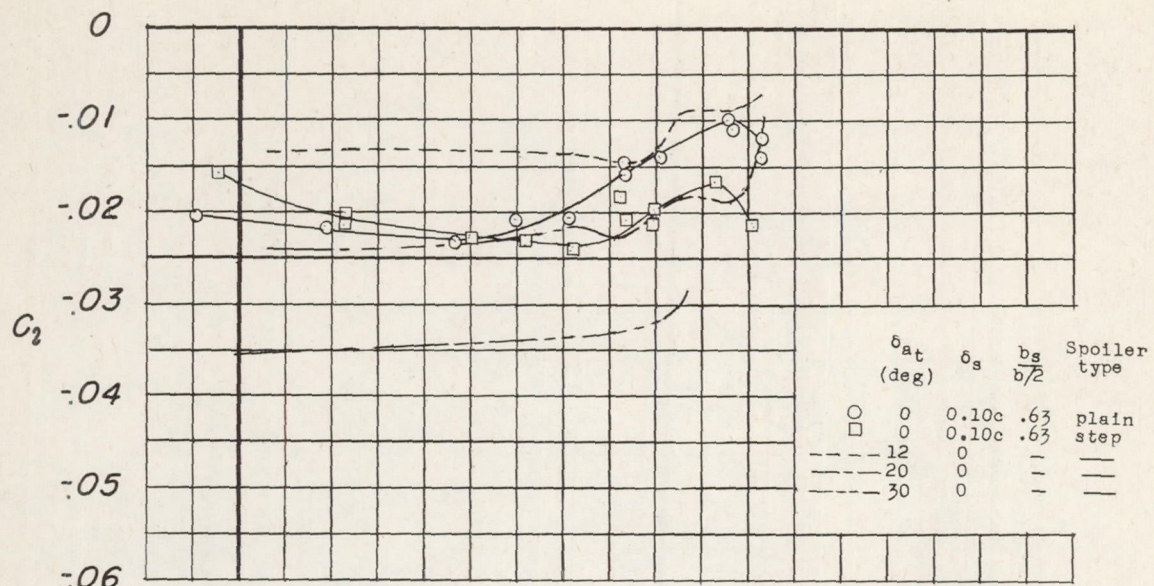
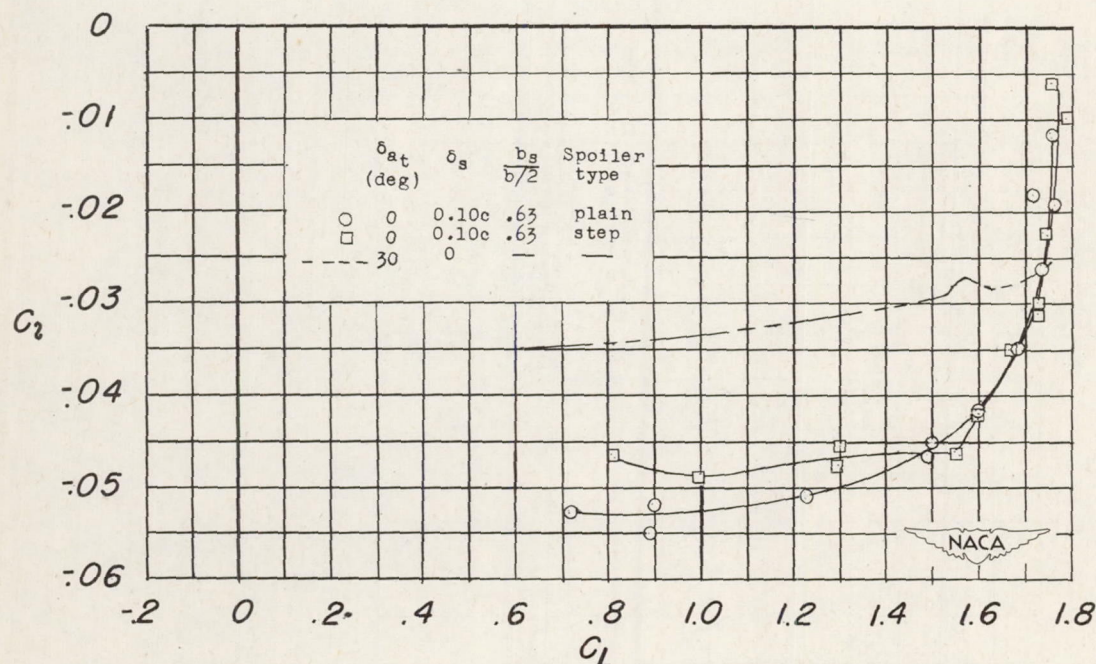
(c) Lift and pitching moment; outboard spoiler;  $\delta_s = 0.10c$ .

Figure 13.- Concluded.



(a) Flaps neutral.



(b) Leading-edge flap and double slotted flap deflected.

Figure 14.- Comparison of aileron and outboard spoiler on a  $32^\circ$  sweptforward wing with fuselage.